# Complementing regional moment magnitudes to GCMT: a perspective from the rebuilt ISC Bulletin

Domenico Di Giacomo[1,*], James Harris[1], and Dmitry A. Storchak[1]

[1]International Seismological Centre (ISC), Pipers Lane, Thatcham, Berkshire, RG19 4NS, United Kingdom

**Correspondence:** Domenico Di Giacomo (domenico@isc.ac.uk)

**Abstract.** Seismologists and geoscientists in general often need earthquake catalogues for various types of research. This input usually contains basic earthquake parameters such as location (longitude, latitude, depth and origin time) as well as magnitude information. For the latter, the moment magnitude $Mw$ has became the most sought after magnitude scale in the seismological community to characterize the size of an earthquake. In this contribution we provide an informative account of the $Mw$ content for the newly rebuilt Bulletin of the International Seismological Centre (ISC, www.isc.ac.uk), which is regarded as the most comprehensive record of the Earth's seismicity. From it, we extracted a list of hypocentres with $Mw$ from a multitude of agencies reporting data to the ISC. We first summarize the main temporal-spatial features of the $Mw$ provided by global agencies (i.e., providing results for moderate to great earthquakes worldwide) and regional ones (i.e., also providing results or small earthquakes in a specific area). Then we discuss their comparisons, not only by considering $Mw$ but also the surface wave magnitude $MS$ and short-period body wave magnitude $mb$. By using the Global Centroid Moment Tensor solutions as authoritative global agency, we identify regional agencies that best complement it and show examples of frequency-magnitude distributions in different areas obtained both from the Global Centroid Moment Tensor alone and complemented by $Mw$ from regional agencies. The work done by the regional agencies in terms of $Mw$ is fundamental to improve our understanding of the seismicity of an area and we call for the implementation of procedures to compute $Mw$ in a systematic way in areas currently not well covered in this respect, such as vast parts of continental Asia and Africa. In addition, more studies are needed to clarify the causes of the apparent overestimation of global $Mw$ estimations compared to regional $Mw$. Such difference is also observed in the comparisons of $Mw$ with $MS$ and $mb$. The results presented here are obtained from the dataset (Di Giacomo and Harris, 2020, https://doi.org/10.31905/J2W2M64S) stored at the ISC Dataset Repository (www.isc.ac.uk/dataset_repository/).

## 1 Introduction

Among the different magnitude scales developed over the years to measure an earthquake's size, the moment magnitude $Mw$ introduced by Kanamori (1977) and Hanks and Kanamori (1979) has a fundamental role in seismology. It is considered the most reliable and, as such, the reference earthquake magnitude in different areas of research in seismology and geophysics (e.g., earthquake source studies, tsunamis, tectonics and geodynamics) and related applications (e.g., ground-motion prediction equations, site effects and seismic hazard). Its computation relies on reliable estimimation of the scalar seismic moment $M_0$ (Aki, 1966) via the relationship (e.g., IASPEI, 2013): $Mw = \frac{2}{3} \cdot (\log_{10} M_0 - 9.1)$, with $M_0$ given in Nm.

Since its introduction many research groups developed techniques to routinely compute *Mw* for monitoring and/or research purposes. Some seismological agencies systematically compute *Mw* on a global scale and, in recent years, more at regional scale (i.e., magnitude 5 and below in a specific area). As part of the mission of the International Seismological Centre (ISC, www.isc.ac.uk) to collect, integrate, review and reprocess seismic bulletins from seismological agencies around the world, the ISC Bulletin (International Seismological Centre, 2020) is, to our knowledge, the most comprehensive resource where researchers interested in *Mw* can combine the information from global agencies and regional ones over several decades (details in the following sections).

With the completion in early 2020 of the Rebuild project (Storchak et al., 2017, 2020) of the ISC Bulletin, here we provide an overview of the *Mw* content in the rebuilt ISC Bulletin and discuss some of its features. In particular, we outline the spatial and temporal properties of *Mw* from global and regional agencies (Section 2) and then discuss their comparisons and characteristics of *Mw* with the ISC re-computed surface wave magnitude *MS* and short-period body-wave magnitude *mb* (Section 3). Finally, we discuss the feasibility of complementing regional *Mw* to global ones by showing the Gutenberg-Richter distribution in some areas where regional *Mw* is available for a long period of time (Section 5).

## 2   *Mw* in the ISC Bulletin

As mentioned earlier, the ISC Bulletin (International Seismological Centre, 2020) contains the *Mw* from a multitude of seismological agencies around the world (readers familiar with the ISC Bulletin content in terms of *Mw* may skip this section and go directly to Section 3). Each agency contributing data to the ISC Bulletin is identified with a code and their details can be found at www.isc.ac.uk/iscbulletin/agencies. The aim of this work is not to outline the different techniques adopted by each agency to compute *Mw*. Such techniques have been extensively documented in scientific literature and readers should refer to the citations (if any available) for more information on the technique of a specific agency.

Without repeating the whole process behind the production of the ISC Bulletin (see, e.g., Section 3 of International Seismological Centre, 2013 for a detailed overview), here we recall that the ISC, to begin with, groups the reported hypocentres and related data (e.g., arrival times, amplitudes, nodal planes, moment tensors etc.) by physical event. Then, usually 24 to 30 months behind real-time, the ISC analysts review the Bulletin (on a monthly batch basis) by assessing the location and magnitude (Bondár and Storchak, 2011) of the largest events (normally events with a magnitude above 3.5) and running a series of checks, some of which include the unreviewed events (e.g., events too small and often reported by a single agency). During the review process, among other changes, events may be banished, merged or split, hypocentres (and possibly related data) may be re-associated or, in exceptional cases, deprecated. The final product is a bulletin containing the ISC relocations (if the event has been relocated) in addition to the results (e.g., hypocentres, centroid locations, magnitudes) of contributing agencies. As such the ISC Bulletin is considered the most comprehensive record of the Earth's seismicity and the starting (raw) dataset for many studies.

The ISC Bulletin 1964-2017 contains over 7 million events, and about 1.9 million of those have been reviewed. As we focus on *Mw* in this work, we extracted from the ISC Bulletin (1964-2017) a list of hypocentres with *Mw* from reporting agencies

(the ISC does not currently compute $Mw$). This dataset is freely available at the ISC Dataset Repository at http://doi.org/10.
31905/J2W2M64S (Di Giacomo and Harris, 2020) and represents the seed input for all results shown in the following sections.
For simplicity, hereafter we refer to this dataset as the "DH $Mw$ List". Details on how we created the list of $Mw$ entries from
the ISC Bulletin as well as the explanation of the parameters included can be found in Section 7. The DH $Mw$ List starts in
1964 (official starting year of the ISC) and stops in 2017 (coinciding with the last complete calendar year of the reviewed ISC
Bulletin at the time of writing). $Mw$ are obviously available in the ISC Bulletin from 2018 to present and also before 1964 but
they are not considered here.

The DH $Mw$ List contains 210,929 entries belonging to 179,112 earthquakes. Hence, $Mw$, despite being the preferred magni-
tude scale by the seismological community, is available only for a small fraction of the Earth's seismicity (see also Di Giacomo
and Storchak, 2015). In total, 89 different $Mw$ authors (hereafter we use agency and magnitude author interchangeably) are
included in DH $Mw$ List and their timeline is shown in Fig. 1 . Only a few agencies report $Mw$ systematically or with few
gaps over several years. Those include the solutions at global scale of the Global Centroid Moment Tensors project (GCMT,
www.globalcmt.org, Dziewonski et al., 1981; Ekström et al., 2012), the National Earthquake Information Center of the US
Geological Survey (NEIC, https://earthquake.usgs.gov/earthquakes/search/, e.g., Benz and Herrmann, 2014), and, at regional
scale, the National Research Institute for Earth Science and Disaster Prevention (NIED, https://www.fnet.bosai.go.jp/top.php)
and the Institute of Earth Sciences, Academia Sinica (ASIES, http://www.earth.sinica.edu.tw/, Kao et al., 1998; Kao and Jian,
1999). Also, in the last ~20 years there has been an increase in the agencies reporting $Mw$ to the ISC, particularly in the Amer-
icas. In the following sections we look in more detail at the agencies reporting $Mw$ to the ISC first at global scale and then the
ones operating at regional scale.

## 2.1  $Mw$ from global agencies

The two long-running agencies reporting $Mw$ systematically to the ISC for earthquakes occurring anywhere in the world
are GCMT and NEIC. In addition, after the great Sumatra earthquake of 26 December 2004, many agencies developed fast
procedures to compute $Mw$ soon after the earthquake occurrence. Hence, also other agencies started computing $Mw$ for global
earthquakes. Among such agencies, the Institut de Physique du Globe de Paris (IPGP, http://www.ipgp.fr/, Vallée et al., 2010;
Vallée, 2013) started to report to the ISC. In the following we give a brief summary of the $Mw$ contribution to the ISC Bulletin
of these agencies. Our aim is not to assess the magnitude of completeness of the $Mw$ reporters, but simply to highlight their
main features.

Seismologist are very familiar with the $Mw$ provided by GCMT, and its use is quite common in the scientific literature (see,
e.g., Yoder et al., 2012, for an assessment of GCMT completeness). Fig. 2 is a summary plot showing the GCMT centroid
locations along with the timeline, magnitude histograms and the number of events per year. We will show such a plot for
different agencies to summarize the time and spatial coverage of an agency as well as the $Mw$ range. The GCMT solutions
pre-1976 are only for deep (Huang et al., 1997) and intermediate-depth (Chen et al., 2001) earthquakes, and from 1977 to
2004 it contains mostly earthquakes with $Mw$ 5.0 and above. From 2004-2005 GCMT also computed moment tensors and
$Mw$ for earthquakes down to 4.5 or even lower as obtained from special studies (see Nettles and Hjörleifsdóttir, 2010, and

further references at https://www.globalcmt.org/Events/). Due to its long-term and highly homogenous solutions, GCMT is normally considered the most authoritative *Mw* agency for earthquakes worldwide and used as the reference magnitude in many seismological studies.

Soon after the earthquake occurrence and before the final GCMT solution is available, however, the *Mw* solution of the NEIC, IPGP and others are often used as the reference estimation of an earthquake magnitude. Fig. 3 shows the summary of the NEIC *Mw* available in the ISC Bulletin up to 2017. It has to be pointed out that currently the NEIC may obtain *Mw* using different approaches: the *Mww* (Hayes et al., 2009) from W-phase (Kanamori, 1993) inversion; the *Mwb* from body-wave inversion (based on Ammon et al., 1998, and expanded for teleseismic distances); the *Mwc* from long-period surface wave inversion (see Polet and Thio, 2011, and references therein). In addition, NEIC bulletins may also include the *Mwr* from different contributors as obtained from the inversion of regional recordings (see *Mwr* section at https://earthquake.usgs.gov/data/comcat/data-products.php). The *Mw* from NEIC does not specify the type for earthquake data prior to August 2013 in the ISC Bulletin. In Appendix A are included the summary plots from August 2013 for *Mww* (Fig. A1), *Mwb* (Fig. A2), *Mwc* (Fig. A3) and *Mwr* (Fig. A4). Fig. 3 shows that the NEIC *Mw* solutions increase in number over the years, in particular in the last ten. This is mostly due to the inclusion of *Mwr* (Fig. A4) from different contributors, with *Mwr* available even for earthquakes down to magnitude 3. Differently from the regional contributors we consider in Section 2.2, *Mwr* NEIC is not restricted to a well-defined region, as it is available for earthquakes in the Americas, Euro-Mediterranean area and other parts of Asia and the Pacific ocean.

Fig. A5 in Appendix A shows the summary plots for IPGP, which reports earthquakes with magnitude 5.8 and above, pre-dominantly from subduction zones.

We point out that also the Geophysical Survey of Russian Academy of Sciences (MOS, http://www.gsras.ru/new/ssd_news.html, Starovoit and Mishatkin, 2002) computes *Mw* for large earthquakes (5.5 and above, mostly in Asia) However, since the MOS contribution (123 earthquakes in total) is small compared to other global agencies, we do not include MOS in the discussion. The comparison between *Mw* from GMCT, NEIC and IPGP will be discussed in Section 3.

## 2.2 *Mw* from regional agencies

At regional scale several agencies report *Mw* during different periods (Fig. 1) and in different parts of the world (Fig. 4). The bounding boxes of Fig. 4 are drawn from the hypocentres included in the DH *Mw* List and are not meant as limits of the area investigated by an individual agency. For sake of brevity here we do not include summary plots for each agency (as shown in Fig. 2) but give priority to major regional contributors currently active. However, readers interested in reproducing the summary plot for a specific agency or magnitude author can use the the DH *Mw* List and the script available in Di Giacomo and Harris (2020). More details to this regard are given in Section 7.

In North America, the major regional reporters to the ISC include the Canadian Hazards Information Service, Natural Resources Canada (agencies PGC and OTT, http://www.earthquakescanada.nrcan.gc.ca/index-eng.php, Fig. A6), the University of Alaska (UAF, http://www.uaf.edu/geology/research/seismology-geodesy/), and, via NEIC reports, Saint Louis University (SLM, http://www.eas.slu.edu/Department/department.html, Herrmann et al., 2011), Berkeley Seismological Laboratory (BRK

and NCEDC, http://seismo.berkeley.edu/seismo/, hereafter referred to as BRK/NCEDC), California Institute of Technology (PAS, http://www.seismolab.caltech.edu/), and the Servicio Sismológico Nacional, Mexico (MEX, http://www.ssn.unam.mx/, Pérez-Campos et al., 2019), which resumed reporting *Mw* in 2017.

130     In the Caribbean and Central America, among the agencies actively reporting *Mw* to the ISC is the Instituto Nicaraguense de Estudios Territoriales (INET, http://www.ineter.gob.ni/, now reporting as CATAC, http://catac.ineter.gob.ni/, Fig. A7), Universidad de Panama (UPA, http://www.geocienciaspanama.org/informacion-general-2, Fig. A8) and Universidad de Costa Rica (UCR, http://www.rsn.ucr.ac.cr/, Fig. A9).

        In South America major contributors are the Red Sismológica Nacional de Colombia (RSNC, https://www.sgc.gov.co/, Fig. A10), Fundación Venezolana de Investigaciones Sismológicas (FUNV, http://www.funvisis.gob.ve/, Fig. A11), Centro Sismológico Nacional, Universidad de Chile (GUC, http://www.csn.uchile.cl/, Fig. A12) and Instituto Nacional de Prevención Sísmica (SJA, http://www.inpres.gov.ar/, Sánchez et al., 2013, Fig. A13).

        In the European-Mediterranean area, several agencies over the years reported *Mw* to the ISC (not all shown in Fig. 4). Among the active *Mw* reporters, the most continuous is the European-Mediterranean Regional Centroid-Moment Tensors (MED_RCMT, http://rcmt2.bo.ingv.it/, Pondrelli, 2002, Fig. 5), which largely overlaps both in space and time with currently reporting agencies (AFAD, http://www.deprem.gov.tr/, Alver et al., 2019; BER, http://www.geo.uib.no/seismo/, Ottemöller et al., 2018; ROM, http://www.ingv.it/, Scognamiglio et al., 2006) and other agencies currently not reporting to the ISC (e.g., ZUR_RMT, IPRG and GII, ATA, NIC). The *Mw* from the Instituto Andaluz de Geofisica (IAG, http://www.ugr.es/~iag/, Stich et al., 2003, 2006, 2010; Martín et al., 2015) and GEOMAR (GEOMR, https://www.geomar.de/, Grevemeyer et al., 2015) have been included after the Rebuild project of the ISC Bulletin (Storchak et al., 2017, 2020) from results in journal publications.

        With the exception of North African earthquakes reported by MED_RCMT, no active regional agency is reporting *Mw* to the ISC in most of Africa. Past contributions come from the work of Hofstetter and Beyth (2003, and references therein, in the ISC Bulletin under agency AFAR), and the Council for Geoscience in South Africa (PRE, https://www.geoscience.org.za/) for 2003-2005.

150     In Asia, the two largest and continuous *Mw* contributors are NIED (Fig. 6) for the Japanese archipelago and ASIES (Fig. 7) for the Taiwan island region. Smaller contributions in terms of *Mw* come from the National Centre for Seismology (NDI, https://seismo.gov.in/) for the Indian subcontinent (Fig. A14) and the Badan Meteorologi, Klimatologi dan Geofisika (DJA, https://www.bmkg.go.id/gempabumi/gempabumi-terkini.bmkg?lang=EN for the Indonesian archipelago (Fig. A15). These last two agencies started to contribute more systematically since August 2017 and January 2017, respectively.

155     In Oceania, the only regional contributor is the Institute of Geological and Nuclear Sciences (WEL, http://www.gns.cri.nz/), mostly for the area surrounding New Zealand's North and South islands (Fig. A16).

        Overall, the contribution of regional agencies to the ISC is important for expanding the *Mw* data for earthquakes not usually considered by global agencies (i.e., about magnitude 5 and below). We have seen that regional agencies can cover from relatively small areas (e.g., BRK/NCEDC, PAS, UAF) to large ones (e.g., NIED, SLM, SJA, MED_RCMT) and that from a temporal point of view many more regional agencies started computing *Mw* in the last 10-20 years, although gaps are present and some agencies stopped reporting or are no longer active.

In the context just described, we give special attention in the following sections to NIED and ASIES in Asia, MED_RCMT in the European-Mediterranean region and the above mentioned agencies in the Americas that currently report *Mw* to the ISC.

## 3 *Mw* comparisons

165 In this section we show the comparisons between *Mw* GCMT (as the most homogenous and long-running agency for global earthquakes) with NEIC and selected regional agencies. The aim of such comparisons is to show the variability in *Mw* estimates for global and regional events. The figures shown in the following also include the orthogonal regression (e.g., Bormann et al., 2007, and references therein). The regression results from this work are not meant to be used as authoritative formulas for magnitude conversions but are only shown for guidance to highlight similarities and/or the most significant differences in the

170 magnitude comparisons shown here.

### 3.1 *Mw* GCMT and *Mw* NEIC

As shown in Section 2, NEIC can report different types of *Mw*: *Mww*, *Mwb*, *Mwc*, *Mwr*. However, only with data starting in August 2013 do the NEIC reports to the ISC specify in the *Mw* type the procedure used to obtain it. For this reason, we compare *Mw* GCMT and NEIC before August 2013 (generic *Mw*) and from August 2013 for NEIC *Mww*, *Mwc* and *Mwb* (Fig. 8). The

175 comparison with *Mwr* will be included in Section 3.3.6. Overall, the agreement between GCMT and NEIC *Mw* is very good, both in the period 1980-2013/07 and 2013/08-2017, as the average difference is within 0.1 magnitude units (m.u.) with 0.1 standard deviation. However, some features can still be seen, as already pointed out by Gasperini et al. (2012). Indeed, Fig. 8 shows how GCMT and NEIC agree well particularly in the magnitude range 5 to 7, whereas GCMT, with a few exception, is marginally larger than NEIC for earthquakes below 5 and above 7. In recent years, however, Fig. 8 shows how NEIC and

180 GCMT *Mw* fit each other very well, particularly for what concerns NEIC's *Mww*, *Mwc* and *Mwb*.

### 3.2 *Mw* GCMT and *Mw* IPGP

The need for promptly computing *Mw* after an earthquake to assess its impact, particularly in terms of its tsunami potential, resulted in the implementation of fast procedures to compute *Mw* for earthquakes worldwide at the IPGP. Fig. A17 shows the comparison between *Mw* from GCMT and IPGP. The *Mw* from IPGP shows a slightly larger values than GCMT, at times by

185 up to 0.4 m.u. However, IPGP in general follows GCMT well along the 1:1 line and is confirmed to be an important asset for the community when it comes to rapidly assessing *Mw*.

### 3.3 *Mw* GCMT and *Mw* from regional agencies

Since the *Mw* from global agencies shows very good agreement at global level, here we use the authoritative *Mw* from GCMT for the comparisons with *Mw* from regional agencies. We start with *Mw* from active agencies in the Americas (North, Central

190 and South), before the Euro-Mediterranean area and the areas around Japan (agency NIED) and Taiwan island (agency ASIES). Finally, we give a quick overview for other agencies. Agencies from the Caribbean (SDD, JSN, SSNC) have insufficient data

to create comparisons with GCMT as well as *mb* and *MS* from the ISC. Therefore we do not include Caribbean agencies in the following sections. As GCMT provides *Mw* mostly for earthquakes with magnitude 5.0 and above (see Fig. 2), the *Mw* shown in the following comparisons are mostly for moderate (i.e., *Mw* between 5 and 6) to great (i.e., *Mw* 8+) earthquakes. The comparisons shown here also serve to establish a hierarchy in the preference of regional agencies when there are spatial overlaps, such as in Central America (see Fig. 4). We will make use of such preferences in Section 5.

### 3.3.1 North America

Among the the regional agencies reporting *Mw* to the ISC in North America (Fig. 4), we show the comparisons with *Mw* GCMT for agencies PGC/OTT, BRK/NCEDC, PAS and SLM. We do not consider in this section UAF and MEX as we have only a few events in common with GCMT from the DH *Mw* List. Fig. 9 shows that, overall, *Mw* GCMT is marginally (about 0.1 m.u.) larger than *Mw* from North American agencies. Agencies PAS and BRK/NCEDC show a good agreement with GCMT as the orthogonal regression closely follows the 1:1 line, although with an average difference of about 0.1 m.u., whereas for PGC/OTT the scatter is larger, particularly for moderate earthquakes and below, and SLM seems offset by -0.1 m.u. from GCMT. For North America therefore the regional *Mw* preference is PAS with BRK/NCEDC, followed by PGC/OTT.

### 3.3.2 Central America

Among the the regional agencies reporting *Mw* to the ISC in Central America (Fig. 4), we show the comparisons with *Mw* GCMT for agencies INET/CATAC, UCR and UPA. Fig. 10 shows large differences between *Mw* GCMT and *Mw* from INET/CATAC and UCR. Agency UPA shows a better agreement with GCMT (~14% of the GCMT - UPA *Mw* values differ by more than ±0.5 m.u.), although large differences of about 1 m.u. can occur. Agency INET/CATAC has a significant average difference with GCMT of about 0.4 m.u., whereas UCR shows a distribution similar to PGC/OTT but with larger scatter and variability (average difference = 0.2 m.u.). For this area, we will use the results from agency UPA in the following sections.

### 3.3.3 South America

Among the the regional agencies reporting *Mw* to the ISC in Central America (Fig. 4), we show the comparisons with *Mw* GCMT for agencies RSNC, FUNV, GUC and SJA. Agency SCB has only 4 earthquakes in common with GCMT and is therefore not discussed here. The *Mw* comparisons shown in Fig. 11 highlights a good fit between GCMT and the Chilean agency GUC for the whole magnitude range. Agency SJA, which largely overlaps with GUC, shows significant deviations from GCMT in the whole magnitude range. It is more difficult to assess agency RSNC and FUNV for paucity of data (total number of points = 60 and 56, respectively). However, we note that RSNC shows a scatter similar to PGC/OTT for moderate earthquakes and agrees well with GCMT for strong (*Mw* between 6 and 7) to major (*Mw* between 7 and 8) earthquakes, whereas FUNV shows a larger scatter. Since the areas considered by GUC and SJA as well as RSCN and FUNV overlap to some extent, we give preference to GUC over SJA and to RSNC over FUNV.

## 4  Comparisons of *MS* and *mb* from the ISC with *Mw*

250

We have seen in previous sections that *Mw* GCMT and several regional *Mw* providers fit well for strong and major earthquakes, whereas for moderate and smaller earthquakes the variability of the differences between GCMT and regional *Mw* values is higher, with GCMT nearly always larger than regional *Mw* values. This observation is not new as, for example, Patton (1998) and Patton and Randall (2002) showed the tendency of GCMT to overestimate seismic moments (hence of *Mw*) in central

255   Asia, particularly for lower magnitude earthquakes. It is not the scope of this work to further investigate the reasons for such differences (see, e.g., Hjörleifsdóttir and Ekström, 2010), as our main aim is to highlight large features of the *Mw* from the ISC Bulletin as an instrumental resource for further research into *Mw*.

Fig. 2 shows how GCMT, although it is the authoritative agency for global earthquakes, is not systematically computing *Mw* for earthquakes below 5. Therefore, to further assess the variability of the regional *Mw* providers at lower magnitudes, we use

260   the ISC re-computed *MS* and *mb* (Bondár and Storchak, 2011).

The global comparisons between GCMT *Mw* and ISC re-computed *MS* and *mb* have been extensively discussed in literature. In Fig. 13 and Fig. 14 we show, for each regional agency discussed in previous sections, the comparisons between ISC re-computed *MS* and *mb*, respectively, with GCMT and each regional agency (the only difference here is that we grouped PAS with BRK/NCEDC). The global comparisons between GCMT *Mw* and ISC re-computed *MS* and *mb* have been extensively

265   discussed in literature. Therefore, Fig. 13 and Fig. 14 only include GCMT *Mw* values for earthquakes that occurred in the same area of the corresponding regional agency (see Fig. 4 for the spatial limits of each agency).

Fig. 13 and Fig. 14 also show the non-linear regressions between ISC magnitudes and GCMT as well as regional *Mw* agencies. The non-linear regressions have been computed similarly to Di Giacomo et al. (2015), with the difference being that in this work we did not use a global dataset split in training and validation subsets. Other non-linear models have been proposed

270   by Lolli et al. (2014) but, as we do not aim to create new conversion relationships, we only use our non-linear regressions to discuss features of the ISC re-computed *MS* and *mb* with GCMT and regional agencies.

The non-linear models for regional agencies shown in Fig. 13 and Fig. 14, obtained with the same regression technique, serve us a sort of guideline for earthquakes below 6 in particular, as for large earthquakes the *MS* and *mb* relations with *Mw* have been studied by several authors (e.g., see Bormann et al., 2013, for a comprehensive overview on the subject).

275   Several papers have shown that *MS* scales with *Mw* better than *mb* for strong and larger earthquakes (e.g., Scordilis, 2006). This is also confirmed by inspecting Fig. 13. Indeed, the *MS* ISC and *Mw* GCMT distribution shows how the non-linear model follows close the 1:1 line for the magnitude range 6.0 to 7.7, whereas for great earthquakes *MS* tends to underestimate *Mw* (Kanamori, 1983) and deviates even more significantly from the 1:1 line going down in magnitude for moderate and smaller earthquakes (see also Bormann et al., 2009). Similar trends can be seen for agencies MED_RCMT, NIED, ASIES, PGC/OTT,

280   BRK/NCEDC and PAS, UPA and GUC, although the non-linear models below 6 are much closer to the 1:1 line than the GCMT model. This is not surprising considering the *Mw* comparisons that showed how *Mw* GCMT is generally larger than those agencies for moderate earthquakes and below. Larger deviations are observed for the other agencies. Overall, the regional *MS* - *Mw* distributions appear to complement the global *MS* - *Mw* distribution well, although regional variations are present

(compare, e.g., MED_RCMT and ASIES), as already pointed out by Ekström and Dziewonski (1988). The difference between

285   *MS* ISC and *Mw* GCMT and all other agencies is also shown as box-and-whisker plot for bins of 0.2 m.u. of *MS* ISC (last subplot in Fig. 13). Despite the large scatter of *Mw* shown by regional agencies, such differences become progressively larger as the magnitude decreases.

    The comparison between *mb* ISC and *Mw* GCMT is characterized by a large scatter in the whole magnitude range and shows stronger features compared to *MS*. Indeed, due to the early saturation of *mb* already for strong to major earthquakes

290   (e.g., Kanamori, 1983), *Mw* is, in general, significantly larger than *mb*. This feature is well documented in the literature, hence we focus on the significant difference between GCMT and the other agencies for lower magnitude earthquakes. Indeed, whilst the GCMT distribution with *mb* is strongly non-linear, for all other agencies the non-linear models are much closer to the 1:1 line than the GCMT curve. In particular, agencies MED_RCMT and ASIES appear to extend nearly linearly the *mb* - *Mw* global distribution from the GCMT. Similar trends can be noticed for NIED and PGC/OTT, although with a larger scatter,

295   whereas for other agencies the number of data points are significantly smaller and the regional *mb* - *Mw* distribution appears to complement the global *mb* - *Mw* distribution less clearly. As for *MS*, we observe a significant difference between *mb* - *Mw* from GCMT and all other agencies for smaller earthquakes (last subplot in Fig. 14).

## 5   Examples of frequency-magnitude distributions

As one of the possible uses of the ISC Bulletin as a source of *Mw*, Fig. 15 shows the frequency-magnitude distributions (FMD)

300   for GCMT alone and GCMT complemented by regional agencies discussed above. The FMDs are normally used in many hazard studies and are fundamental in catalogue based assessments of the magnitude of completeness *Mc* for an area in a given time period. The FMDs have been obtained for the time period covered both by GCMT and the corresponding regional agency, as also outlined in the magnitude timelines of Fig. 15. The choice of the agency that best complement GCMT in a specific area has been discussed in previous sections. Fig. 15 also shows *Mc* estimations by two different methods, the median-based analysis

305   of the segment slope by Amorese (2007) and the goodness-of-fit test by Wiemer and Wyss (2000). Other methods for estimating *Mc* are available (see, e.g., Mignan and Woessner, 2012), but here we only use these two methods to provide two independent estimations of *Mc* for GCMT and GCMT complemented by a regional agency. Overall, the effect of complementing the *Mw* from a regional agency with GCMT is to improve the *Mc* for an area, with the exception of Chile where the recent contribution by the regional agency GUC does not, yet, expand significantly the GCMT contribution.

310   We note significant fluctuations in the FMDs for all agencies shown for the Americas, as, for example, in California and neighbouring regions (agencies PAS/BRK-NCEDC), as also shown by the large discrepancy between the *Mc* from the goodness-of-fit test and median-based analysis of the segment slope methods. Agencies NIED, ASIES and MED_RCMT extend to lower magnitudes the GCMT's FMDs better than other agencies. Such FMD examples further emphasize the important role of regional agencies in complementing global solutions (e.g., from GCMT).

## 6 Conclusions

The ISC Bulletin, in its rebuilt shape after the work described in Storchak et al. (2017, 2020), is a unique resource for seismological and multidisciplinary geoscience studies. In this work we focused on the content and features of the moment magnitude *Mw*, as it is possibly the preferred magnitude scale in the seismological community. The earliest records of *Mw* are for for deep and intermediate-depth earthquakes in the 1960s obtained from special studies by the GCMT group (Huang et al., 1997; Chen et al., 2001). Then, since the formal start in 1976, GCMT (initiated by the University of Harvard, USA, Dziewonski et al., 1981) has become the authoritative global agency providing *Mw* for moderate to great earthquakes. In recent decades other agencies also implemented procedures to compute *Mw* for global earthquakes (e.g., NEIC and IPGC), often due to the need for having a quick but reliable assessment of an earthquake's impact soon after its occurrence (e.g., Hayes et al., 2009; Vallée et al., 2010). We have summarized the main time and spatial features of the global *Mw* providers and by their comparisons we confirm the findings of previous works (e.g., Gasperini et al., 2012). In brief, there is a very good agreement between such agencies for strong to great earthquakes, although minor differences are present.

In recent years, the computation of *Mw* has been expanded to light and smaller earthquakes by a multitude of agencies covering from small areas (i.e., country-wide) or to whole continents. The contributions of regional agencies are fundamental for improving seismicity records of an area. To emphasize this point, Fig. 16 shows the summary of the contribution of regional agencies if we exclude earthquakes with *Mw* from global agencies (the only exception is *Mwr* from NEIC, which is included in the figure). As regional agencies make up about 72% of the earthquakes in the DH *Mw* List, we remark the need for continuous and systematic *Mw* solutions to be provided over a long period of time, as such datasets will be fundamental tools for a better understanding of the seismicity of an area.

The time and spatial summaries of the regional agencies highlighted the recent increase in *Mw* providers, although the agencies currently active and having few interruptions in their contributions are located mostly in North America, Euro-Mediterranean, Japanese archipelago and Taiwan areas. Unfortunately, large parts of the world with significant seismicity (e.g., vast parts of continental Asia and Africa) lack regional agencies reporting *Mw* (see Fig. 4 and Fig. 16).

The *Mw* comparisons between GCMT and regional agencies showed a feature already discussed in literature, that is a growing deviation from the 1:1 line for moderate to smaller earthquakes. Such deviation is usually accompanied by a larger scatter in the data points compared to earthquakes in higher magnitude ranges (e.g., magnitude 6 and above). These observations are not limited to a specific area but appear to be common in different parts of the world. In addition, the GCMT *Mw* comparisons with the ISC-recomputed magnitudes, *MS* and *mb*, confirm such discrepancies. Indeed, GCMT appears nearly systematically larger than regional ones for earthquakes in the same area below about magnitude 5.5, as highlighted by the nonlinear regressions shown in this work. Nearly all deviate from the 1:1 line more significantly for GCMT than corresponding models for regional agencies.

When multiple agencies overlap in space and time, we used magnitude comparisons to select individual regional agencies that better complement GCMT in a given area. This way we discussed examples of frequency-magnitude distributions from GCMT alone and GCMT complemented by specific regional agencies in different parts of the world. It is not surprising that by

complementing GCMT with the *Mw* of a regional agency we have shown improvements in *Mc* estimations. The best examples
350  of extending the GCMT FMDs to smaller magnitudes are from agencies MED_RCMT, NIED and ASIES, whereas in other
areas the GCMT as well as the GCMT complemented by regional agencies show marked fluctuations. Although we did not
aim to investigate in detail the frequency-magnitude distributions, a possible source of such fluctuations, e.g. for California,
may be due to the short time window considered. Hence, we encourage agencies to continue or implement procedures for
systematically computing *Mw* for the years to come, so that future works may benefit from long-running and homogenous
355  datasets.

Finally, we point out that further investigations on the difference between *Mw* from GCMT and regional agencies are desir-
able, although several papers (e.g., Patton, 1998; Patton and Randall, 2002; Hjörleifsdóttir and Ekström, 2010; Konstantinou
and Rontogianni, 2011) considered this aspect. Addressing such discrepancies may have significant impacts in different types
of studies (e.g., magnitude conversion relationships, ground-motion prediction equations, hazard, etc.). In particular, we envis-
360  age studies that estimate the effects of possible data censoring in *Mw* computations in different regions, which may explain,
even partially, the growing deviations from the 1:1 lines between *Mw* GCMT and *mb*|*MS* in the lower magnitude ranges.

## 7  Code and data availability

The DH *Mw* List (filename = MW_all_1964-2017, Di Giacomo and Harris, 2020) is available in the ISC Dataset Repository
at http://doi.org/10.31905/J2W2M64S. It has been extracted from the ISC Bulletin (International Seismological Centre, 2020)
365  and each line contains the following fields (as in the file header line):
event type (*etype*), ISC event identifier (*isc_evid*), hypocentre identifier (*hypid*), hypocentre author (*h.author*), hypocentre
author origin time (*OT*), hypocentre author latitude (*lat*), hypocentre author longitude (*lon*), hypocentre author depth (*depth*),
magnitude type (*mtype*), magnitude author (*n.author*), magnitude (*mag*), magnitude uncertainty (*unc*), data provider (*reporter*),
magnitude identifier (*magid*), prime location author (*prime*), absolute depth difference between *h.author* and *prime* (*Hdiff*, in
370  km), epicentral distance between *h.author* and *prime* (*dist*, in km).
The database identifiers (*isc_evid*, *hypid* and *magid*) are included for facilitating identification of entries from users. Note that
for the same event (i.e., one *isc_evid*) there can be from 1 to *N hypid* and *magid* entries. For some entries the *n.author* is
different from the *h.author* as some reporters (e.g., NEIC) often provide magnitude values from third parties.

The entries included in the DH *Mw* List, as extracted from the ISC Bulletin, include only the following *mtype* (case insensi-
375  tive):
*Mw*, *Mwb*, *Mwc*, *Mwr*, *Mww*. This means that *Mw* computed for rapid response purposes, such as *Mwp* (Tsuboi et al., 1995,
1999; Tsuboi, 2000), *MwMwp* (Whitmore et al., 2002), *Mwpd* (Lomax et al., 2007) or proxy values such as *Mw(mB)* (Bormann
and Saul, 2008), have been skipped.

Other *Mw* entries in the ISC Bulletin not included in the DH *Mw* List are those with associated uncertainty larger than 0.5
380  (note that *unc* = 0 means no formal uncertainty is associated to the magnitude value). Finally, with the exception of *Mw* from
GCMT, we skipped *Mw* entries where *dist* is larger than 300 km and *Hdiff* > 150 km.

Below are the Perl lines used to write out the DH *Mw* List:

```
$str = sprintf "%s %12d %12d %8s %s %9.3f %10.3f %6.1f %6s %12s %4.2f %3.1f %12s
     %12d %8s %8.1f %8.1f\n",
$etype, $evid, $hypid, $hauthor, $ot, $lat, $lon, $depth, $mtype, $nauthor,
     $magnitude, $unc, $reporter, $magid, $primeauthor, $diffdepth, $deltakm ;

print OUT ("$str") ; # OUT is the DH Mw List in the manuscript, file name =
     MW_all_1964−2017 in the ISC Dataset Repository, doi: 10.31905/J2W2M64S
```

In Di Giacomo and Harris (2020) we also include the Generic Mapping Tools (GMT4.5, Wessel et al., 2013) script to create the summary plots (as in Fig. 2 or Fig. 5 for any magnitude author the user may wish to visualize, as mentioned in Section 2.2).

Finally, users can find in dedicated subfolders (see README file in Di Giacomo and Harris, 2020) the files used to create the magnitude comparisons shown in this work.

395  *Author contributions.*  DDG is the lead author and prepared the dataset and figures. JH maintains the database and ISC web services, and DAS obtained the funding for the work and established and maintained connections with many data providers. All the authors contributed to the manuscript and approved the final version.

*Competing interests.*  The authors declare that they have no conflict of interest

*Acknowledgements.*  We are grateful to all reporters that contribute or have contributed data to the ISC, particularly in terms of *Mw* for this
400  work. The work done at the ISC is possible thanks to the support of its members (http://www.isc.ac.uk/members/, last access: December 2020) and sponsors (http://www.isc.ac.uk/sponsors/, last access: December 2020). Work partially funded by NSF grants 1811737, 1417970 and 0949072; USGS Awards G14AC00149, G15AC00202, G18AP00035 and G19AS00033. All figures were drawn using the Generic Mapping Tools (Wessel et al., 2013).

# References

405    Aki, K.: Generation and Propagation of G Waves from the Niigata Earthquake of June 16, 1964. Part 2. Estimation of earthquake moment, released energy, and stress-strain drop from the G wave spectrum, Bulletin of the Earthquake Research Institute, University of Tokyo, 44, 73–88, http://hdl.handle.net/2261/12237, 1966.

Alver, F., Ömer Kılıçarslan, Kuterdem, K., Türkoğlu, M., and Şentürk, M.: Seismic Monitoring at the Turkish National Seismic Network (TNSN), Summary of the Bulletin of the International Seismological Centre, 53, 41–58, https://doi.org/10.31905/d9grp8rd, 2019.

410    Ammon, C. J., Herrmann, R. B., Langston, C. A., and Benz, H.: Faulting Parameters of the January 16, 1994 Wyomissing Hills, Pennsylvania Earthquakes, Seismological Research Letters, 69, 261–269, https://doi.org/10.1785/gssrl.69.3.261, 1998.

Amorese, D.: Applying a Change-Point Detection Method on Frequency-Magnitude Distributions, Bulletin of the Seismological Society of America, 97, 1742–1749, https://doi.org/10.1785/0120060181, 2007.

Benz, H. M. and Herrmann, R. B.: Rapid Estimates of the Source Time Function and Mw using Empirical Green's Function Deconvolution,
415    Bulletin of the Seismological Society of America, 104, 1812–1819, https://doi.org/10.1785/0120130325, 2014.

Bird, P.: An updated digital model of plate boundaries, Geochemistry, Geophysics, Geosystems, 4, 1027, https://doi.org/10.1029/2001gc000252, 2003.

Bondár, I. and Storchak, D. A.: Improved location procedures at the International Seismological Centre, Geophysical Journal International, 186, 1220–1244, https://doi.org/10.1111/j.1365-246x.2011.05107.x, 2011.

420    Bormann, P. and Saul, J.: The New IASPEI Standard Broadband Magnitude mB, Seismological Research Letters, 79, 698–705, https://doi.org/10.1785/gssrl.79.5.698, 2008.

Bormann, P., Liu, R., Ren, X., Gutdeutsch, R., Kaiser, D., and Castellaro, S.: Chinese National Network Magnitudes, Their Relation to NEIC Magnitudes, and Recommendations for New IASPEI Magnitude Standards, Bulletin of the Seismological Society of America, 97, 114–127, https://doi.org/10.1785/0120060078, 2007.

425    Bormann, P., Liu, R., Xu, Z., Ren, K., Zhang, L., and Wendt, S.: First Application of the New IASPEI Teleseismic Magnitude Standards to Data of the China National Seismographic Network, Bulletin of the Seismological Society of America, 99, 1868–1891, https://doi.org/10.1785/0120080010, 2009.

Bormann, P., Wendt, S., and Di Giacomo, D.: Seismic Sources and Source Parameters, pp. 1–259, Deutsches GeoForschungsZentrum GFZ, https://doi.org/10.2312/GFZ.NMSOP-2_CH3, 2013.

430    Chen, P.-f., Nettles, M., Okal, E. A., and Ekström, G.: Centroid moment tensor solutions for intermediate-depth earthquakes of the WWSSN–HGLP era (1962–1975), Physics of the Earth and Planetary Interiors, 124, 1–7, https://doi.org/10.1016/s0031-9201(00)00220-x, 2001.

Di Giacomo, D. and Harris, J.: An Mw list from the Rebuilt ISC Bulletin (1964-2016), ISC Seismological Dataset Repository, https://doi.org/10.31905/J2W2M64S, 2020.

435    Di Giacomo, D. and Storchak, D. A.: A scheme to set preferred magnitudes in the ISC Bulletin, Journal of Seismology, 20, 555–567, https://doi.org/10.1007/s10950-015-9543-7, 2015.

Di Giacomo, D., Bondár, I., Storchak, D. A., Engdahl, E. R., Bormann, P., and Harris, J.: ISC-GEM: Global Instrumental Earthquake Catalogue (1900–2009), III. Re-computed MS and mb, proxy MW, final magnitude composition and completeness assessment, Physics of the Earth and Planetary Interiors, 239, 33–47, https://doi.org/10.1016/j.pepi.2014.06.005, 2015.

440    Dziewonski, A. M., Chou, T.-A., and Woodhouse, J. H.: Determination of earthquake source parameters from waveform data for studies of global and regional seismicity, Journal of Geophysical Research: Solid Earth, 86, 2825–2852, https://doi.org/10.1029/jb086ib04p02825, 1981.

Ekström, G. and Dziewonski, A. M.: Evidence of bias in estimations of earthquake size, Nature, 332, 319–323, https://doi.org/10.1038/332319a0, 1988.

445    Ekström, G., Nettles, M., and Dziewoński, A. M.: The global CMT project 2004–2010: Centroid-moment tensors for 13,017 earthquakes, Physics of the Earth and Planetary Interiors, 200-201, 1–9, https://doi.org/10.1016/j.pepi.2012.04.002, 2012.

Gasperini, P., Lolli, B., Vannucci, G., and Boschi, E.: A comparison of moment magnitude estimates for the European-Mediterranean and Italian regions, Geophysical Journal International, 190, 1733–1745, https://doi.org/10.1111/j.1365-246x.2012.05575.x, 2012.

Grevemeyer, I., Gràcia, E., Villaseñor, A., Leuchters, W., and Watts, A. B.: Seismicity and active tectonics in the Alboran Sea, Western

450    Mediterranean: Constraints from an offshore-onshore seismological network and swath bathymetry data, Journal of Geophysical Research: Solid Earth, 120, 8348–8365, https://doi.org/10.1002/2015jb012073, 2015.

Hanks, T. C. and Kanamori, H.: A moment magnitude scale, Journal of Geophysical Research, 84, 2348–2350, https://doi.org/10.1029/jb084ib05p02348, 1979.

Hayes, G. P., Rivera, L., and Kanamori, H.: Source Inversion of the W-Phase: Real-time Implementation and Extension to Low Magnitudes,

455    Seismological Research Letters, 80, 817–822, https://doi.org/10.1785/gssrl.80.5.817, 2009.

Herrmann, R. B., Benz, H., and Ammon, C. J.: Monitoring the Earthquake Source Process in North America, Bulletin of the Seismological Society of America, 101, 2609–2625, https://doi.org/10.1785/0120110095, 2011.

Hjörleifsdóttir, V. and Ekström, G.: Effects of three-dimensional Earth structure on CMT earthquake parameters, Physics of the Earth and Planetary Interiors, 179, 178–190, https://doi.org/10.1016/j.pepi.2009.11.003, 2010.

460    Hofstetter, R. and Beyth, M.: The Afar Depression: interpretation of the 1960-2000 earthquakes, Geophysical Journal International, 155, 715–732, https://doi.org/10.1046/j.1365-246x.2003.02080.x, 2003.

Huang, W.-c., Okal, E. A., Ekström, G., and Salganik, M. P.: Centroid moment tensor solutions for deep earthquakes predating the digital era: the World-Wide Standardized Seismograph Network dataset (1962–1976), Physics of the Earth and Planetary Interiors, 99, 121–129, https://doi.org/10.1016/s0031-9201(96)03177-9, 1997.

465    IASPEI: Summary of Magnitude Working Group recommendations on standard procedures for determining earthquake magnitudes from digital data, ftp://ftp.iaspei.org/pub/commissions/CSOI/Summary_WG_recommendations_20130327.pdf, 2013.

International Seismological Centre: Summary of the Bulletin of the International Seismological Centre, January - June 2010, https://doi.org/10.5281/zenodo.998584, 2013.

International Seismological Centre: On-line Bulletin, https://doi.org/10.31905/d808b830, 2020.

470    Kanamori, H.: The energy release in great earthquakes, Journal of Geophysical Research, 82, 2981–2987, https://doi.org/10.1029/jb082i020p02981, 1977.

Kanamori, H.: Magnitude scale and quantification of earthquakes, Tectonophysics, 93, 185–199, https://doi.org/10.1016/0040-1951(83)90273-1, 1983.

Kanamori, H.: W phase, Geophysical Research Letters, 20, 1691–1694, https://doi.org/10.1029/93gl01883, 1993.

475    Kao, H. and Jian, P.-R.: Source Parameters of Regional Earthquakes in Taiwan: July 1995-December 1996, Terrestrial, Atmospheric and Oceanic Sciences, 10, 585, https://doi.org/10.3319/tao.1999.10.3.585(t), 1999.

Kao, H., Jian, P.-R., Ma, K.-F., Huang, B.-S., and Liu, C.-C.: Moment-tensor inversion for offshore earthquakes east of Taiwan and their implications to regional collision, Geophysical Research Letters, 25, 3619–3622, https://doi.org/10.1029/98gl02803, 1998.

Konstantinou, K. I. and Rontogianni, S.: A Comparison of Teleseismic and Regional Seismic Moment Estimates in the European-
480    Mediterranean Region, Seismological Research Letters, 82, 188–200, https://doi.org/10.1785/gssrl.82.2.188, 2011.

Lolli, B. and Gasperini, P.: A comparison among general orthogonal regression methods applied to earthquake magnitude conversions, Geophysical Journal International, 190, 1135–1151, https://doi.org/10.1111/j.1365-246x.2012.05530.x, 2012.

Lolli, B., Gasperini, P., and Vannucci, G.: Empirical conversion between teleseismic magnitudes (mb and Ms) and moment magnitude (Mw) at the Global, Euro-Mediterranean and Italian scale, Geophysical Journal International, 199, 805–828, https://doi.org/10.1093/gji/ggu264,
485    2014.

Lomax, A., Michelini, A., and Piatanesi, A.: An energy-duration procedure for rapid determination of earthquake magnitude and tsunami-genic potential, Geophysical Journal International, 170, 1195–1209, https://doi.org/10.1111/j.1365-246x.2007.03469.x, 2007.

Martín, R., Stich, D., Morales, J., and Mancilla, F.: Moment tensor solutions for the Iberian-Maghreb region during the IberArray deployment (2009–2013), Tectonophysics, 663, 261–274, https://doi.org/10.1016/j.tecto.2015.08.012, 2015.

490    Mignan, A. and Woessner, J.: Estimating the magnitude of completeness for earthquake catalogs, Community Online Resource for Statistical Seismicity Analysis, https://doi.org/10.5078/CORSSA-00180805, 2012.

Mulder, T.: Geological Survey of Canada: Canadian National Seismic Network, Summ. Bull. Internatl. Seismol. Cent., July - December 2011, 48 (7–12), pp. 29–38, Thatcham, United Kingdom, https://doi.org/10.5281/ZENODO.998832, 2015.

Nettles, M. and Hjörleifsdóttir, V.: Earthquake source parameters for the 2010 January Haiti main shock and aftershock sequence, Geophys-
495    ical Journal International, 183, 375–380, https://doi.org/10.1111/j.1365-246x.2010.04732.x, 2010.

Ottemöller, L., Strømme, M. L., and Storheim, B. M.: Seismic Monitoring and Data Processing at the Norwegian National Seismic Network, Summ. Bull. Internatl. Seismol. Cent., 52, 27–40, https://doi.org/10.31905/1m97csyl, 2018.

Patton, H. J.: Bias in the centroid moment tensor for central Asian earthquakes: Evidence from regional surface wave data, Journal of Geophysical Research: Solid Earth, 103, 26 963–26 974, https://doi.org/10.1029/98jb02529, 1998.

500    Patton, H. J. and Randall, G. E.: On the causes of biased estimates of seismic moment for earthquakes in central Asia, Journal of Geophysical Research: Solid Earth, 107, 2302, https://doi.org/10.1029/2001jb000351, 2002.

Pérez-Campos, X., Espíndola, V. H., Pérez, J., Estrada, J. A., Cárdenas Monroy, C., Zanolli, B. F., Bello, D., González-López, A., González Ávila, D., Maldonado, R., Montoya-Quintanar, E., Vite, R., Martínez, L. D., Tan, Y., Rodríguez Rasilla, I., Vela Rosas, M. Á., Cruz, J. L., Cárdenas, A., Navarro Estrada, F., Hurtado, A., and Mendoza Carvajal, A. D. J.: Servicio Sismológico Nacional, Mexico,
505    Summary of the Bulletin of the International Seismological Centre, 53, 29–40, https://doi.org/10.31905/sz7rybtm, 2019.

Polet, J. and Thio, H. K.: Rapid calculation of a Centroid Moment Tensor and waveheight predictions around the north Pacific for the 2011 off the Pacific coast of Tohoku Earthquake, Earth, Planets and Space, 63, 541–545, https://doi.org/10.5047/eps.2011.05.005, 2011.

Pondrelli, S.: European-Mediterranean Regional Centroid-Moment Tensors Catalog (RCMT) [Data Set], Istituto Nazionale di Geofisica e Vulcanologia (INGV), https://doi.org/10.13127/RCMT/EUROMED, 2002.

510    Sánchez, G., Recio, R., Marcuzzi, O., Moreno, M., Araujo, M., Navarro, C., Suárez, J. C., Havskov, J., and Ottemöller, L.: The Argentinean National Network of Seismic and Strong-Motion Stations, Seismological Research Letters, 84, 729–736, https://doi.org/10.1785/0220120045, 2013.

Scognamiglio, L., Tinti, E., and Quintiliani, M.: Time Domain Moment Tensor [Data set], Istituto Nazionale di Geofisica e Vulcanologia (INGV), https://doi.org/10.13127/TDMT, 2006.

515 Scordilis, E. M.: Empirical Global Relations Converting MS and mb to Moment Magnitude, Journal of Seismology, 10, 225–236, https://doi.org/10.1007/s10950-006-9012-4, 2006.

Starovoit, O. and Mishatkin, V.: The seismic network of the Geophysical Survey of the Russian Academy of Sciences, Orfeus newsletter, 4, 1, https://members.noa.gr/g.choul/en/Orfeus2002_vol4no1.pdf, 2002.

Stich, D., Ammon, C. J., and Morales, J.: Moment tensor solutions for small and moderate earthquakes in the Ibero-Maghreb region, Journal
520 of Geophysical Research: Solid Earth, 108, https://doi.org/10.1029/2002jb002057, 2003.

Stich, D., Serpelloni, E., de Lis Mancilla, F., and Morales, J.: Kinematics of the Iberia–Maghreb plate contact from seismic moment tensors and GPS observations, Tectonophysics, 426, 295–317, https://doi.org/10.1016/j.tecto.2006.08.004, 2006.

Stich, D., Martín, R., and Morales, J.: Moment tensor inversion for Iberia–Maghreb earthquakes 2005–2008, Tectonophysics, 483, 390–398, https://doi.org/10.1016/j.tecto.2009.11.006, 2010.

525 Storchak, D. A., Harris, J., Brown, L., Lieser, K., Shumba, B., Verney, R., Di Giacomo, D., and Korger, E. I. M.: Rebuild of the Bulletin of the International Seismological Centre (ISC), part 1: 1964–1979, Geoscience Letters, 4:32, https://doi.org/10.1186/s40562-017-0098-z, 2017.

Storchak, D. A., Harris, J., Brown, L., Lieser, K., Shumba, B., and Di Giacomo, D.: Rebuild of the Bulletin of the International Seismological Centre (ISC) - part 2: 1980–2010, Geoscience Letters, 7:18, https://doi.org/10.1186/s40562-020-00164-6, 2020.

530 Tsuboi, S.: Application ofMwpto tsunami earthquake, Geophysical Research Letters, 27, 3105–3108, https://doi.org/10.1029/2000gl011735, 2000.

Tsuboi, S., Abe, K., Takano, K., and Yamanaka, Y.: Rapid determination of Mw from broadband P waveforms, Bulletin of the Seismological Society of America, 85, 606–613, 1995.

Tsuboi, S., Whitmore, P. M., and Sokolowski, T. J.: Application of Mwp to deep and teleseismic earthquakes, Bulletin of the Seismological
535 Society of America, 89, 1345–1351, 1999.

Vallée, M.: Source time function properties indicate a strain drop independent of earthquake depth and magnitude, Nature Communications, 4, https://doi.org/10.1038/ncomms3606, 2013.

Vallée, M., Charléty, J., Ferreira, A. M. G., Delouis, B., and Vergoz, J.: SCARDEC: a new technique for the rapid determination of seismic moment magnitude, focal mechanism and source time functions for large earthquakes using body-wave deconvolution, Geophysical
540 Journal International, 184, 338–358, https://doi.org/10.1111/j.1365-246x.2010.04836.x, 2010.

Wessel, P., Smith, W. H. F., Scharroo, R., Luis, J., and Wobbe, F.: Generic Mapping Tools: Improved Version Released, Eos, Transactions American Geophysical Union, 94, 409–410, https://doi.org/10.1002/2013eo450001, 2013.

Whitmore, P. M., Tsuboi, S., Hirshorn, B., and Sokolowski, T. J.: Magnitude-dependent correction for Mwp, Science of Tsunami Hazards, 20, 187–192, 2002.

545 Wiemer, S. and Wyss, M.: Minimum Magnitude of Completeness in Earthquake Catalogs: Examples from Alaska, the Western United States, and Japan, Bulletin of the Seismological Society of America, 90, 859–869, https://doi.org/10.1785/0119990114, 2000.

Yoder, M. R., Holliday, J. R., Turcotte, D. L., and Rundle, J. B.: A geometric frequency–magnitude scaling transition: Measuring b=1.5 for large earthquakes, Tectonophysics, 532-535, 167–174, https://doi.org/10.1016/j.tecto.2012.01.034, 2012.
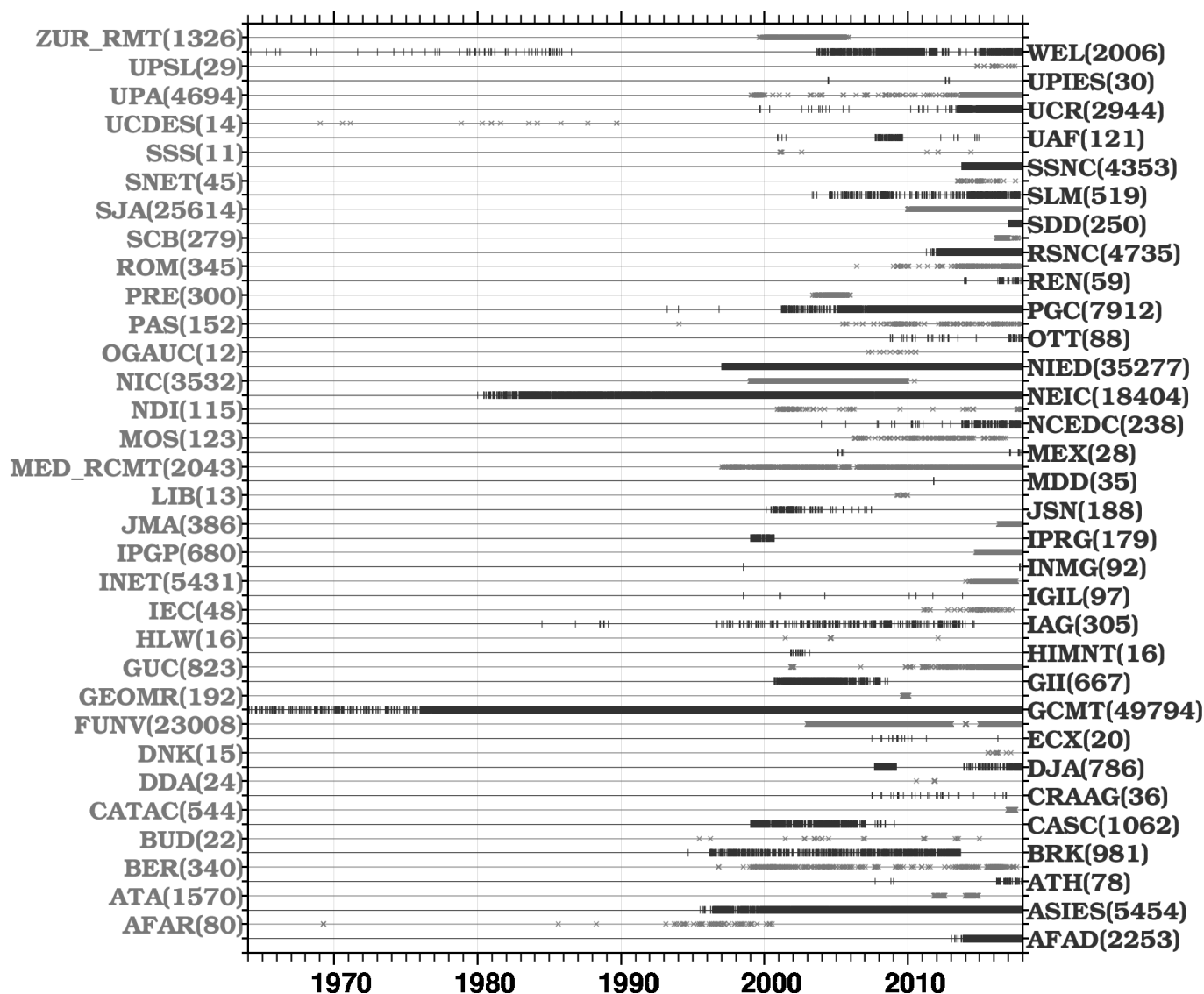
**Figure 1.** Timelines of the agencies contributing with *Mw* to the ISC Bulletin. Details about each agency code can be found by typing the agency code at www.isc.ac.uk/iscbulletin//agencies/. Each symbol represents the origin time of an earthquake and in brackets is the total number of *Mw* for an agency. For better visibility, grey and black text and symbols refer to the agencies listed on the left and on the right, respectively. Note that 25 *Mw* authors with less than 10 entries have been skipped from the DH *Mw* List.
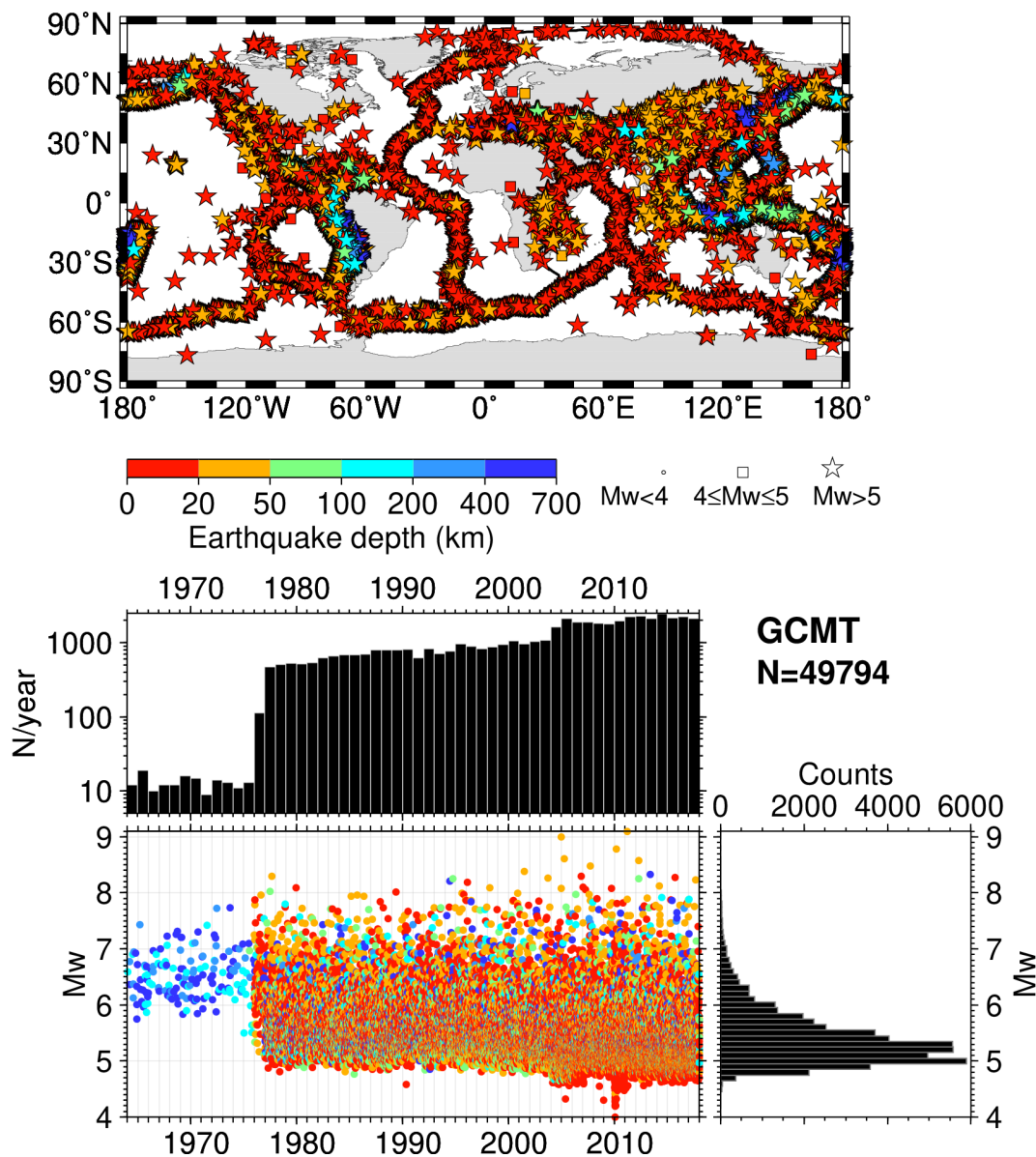
**Figure 2.** Map (top) showing the GCMT centroid location color-coded by depth. Stars are earthquakes with *Mw* greater than 5, squares between 4 and 5, small circles below 4. Although not visible here, the map also includes the Bird (2003) plate tectonic boundaries. The lower panel shows the *Mw* timeline with symbols color-coded by depth along with histograms on the right hand side and number of earthquakes per year on top of the timeline. Only results of special studies for deep (Huang et al., 1997) and intermediate-depth (Chen et al., 2001) earthquakes are available before 1976. The map was drawn using the Generic Mapping Tools (GMT) (Wessel et al., 2013) software.
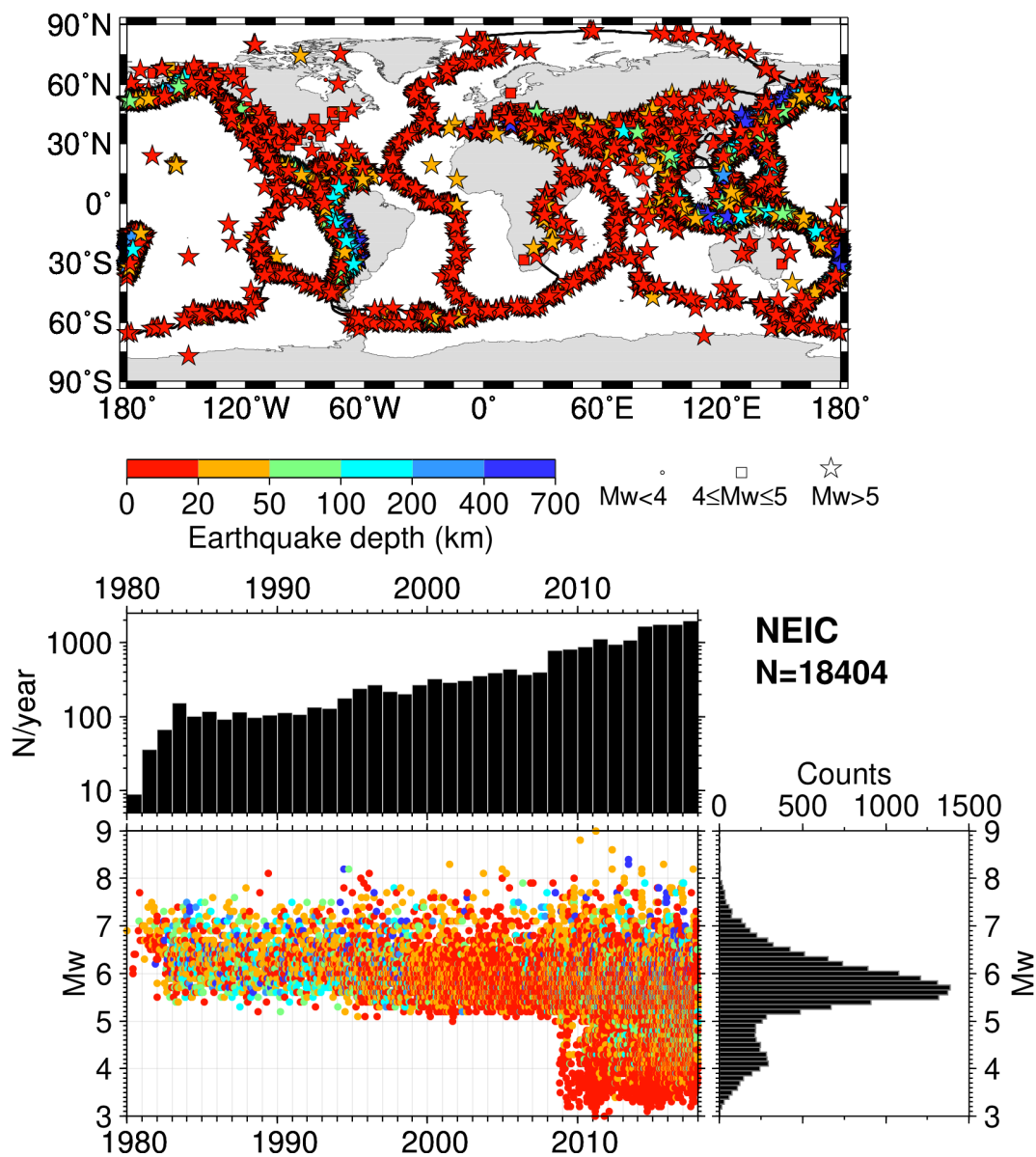
**Figure 3.** As for Fig. 2 but for agency/magnitude author = NEIC. Note that NEIC may compute more than one *Mw* per earthquake, hence the number of *Mw* reported in the Figure here refers to number of *Mw* entries (number of earthquakes = 14,337). See text for details. The map was drawn using the Generic Mapping Tools (GMT) (Wessel et al., 2013) software.
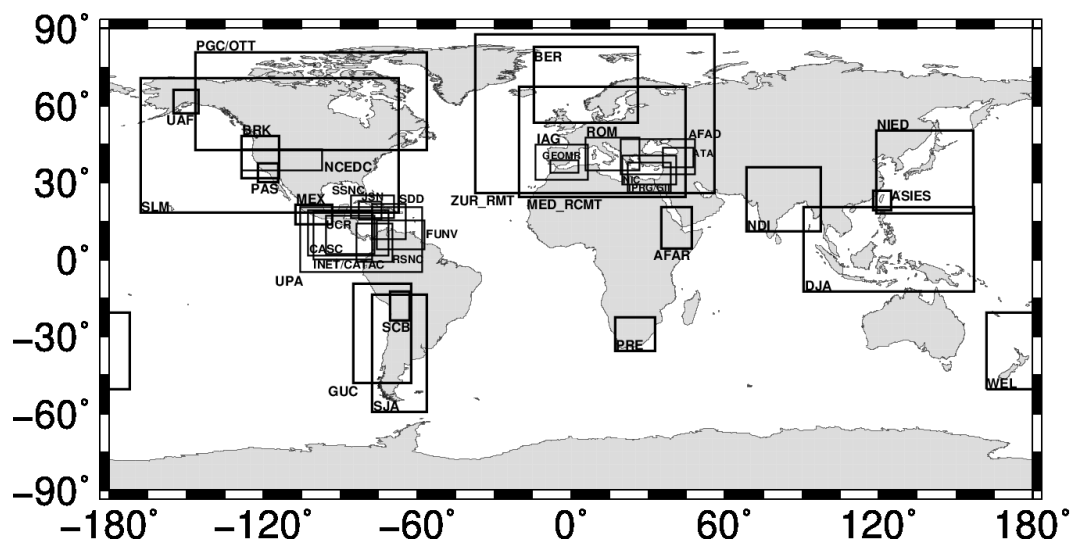
**Figure 4.** Overview of the agencies reporting *Mw* to the ISC at regional scale. For simplicity, only agencies with at leat 100 *Mw* entries are shown (including agencies not reporting, see Fig. 1). Furthermore, JMA is not shown here as it covers the same region of NIED but only starting from 2016. The bounding boxes are retrieved from the hypocentres included in the DH *Mw* List and are not meant as limits of the area monitored by an agency. The boxes are drawn to highlight the regions where *Mw* is available from one or more agencies and areas where *Mw* is available in the ISC Bulletin only from global agencies (e.g., vast parts of Asia, Australia and Africa). The map was drawn using the Generic Mapping Tools (GMT) (Wessel et al., 2013) software.

Open Access  Earth System
Science  Discussions
Data
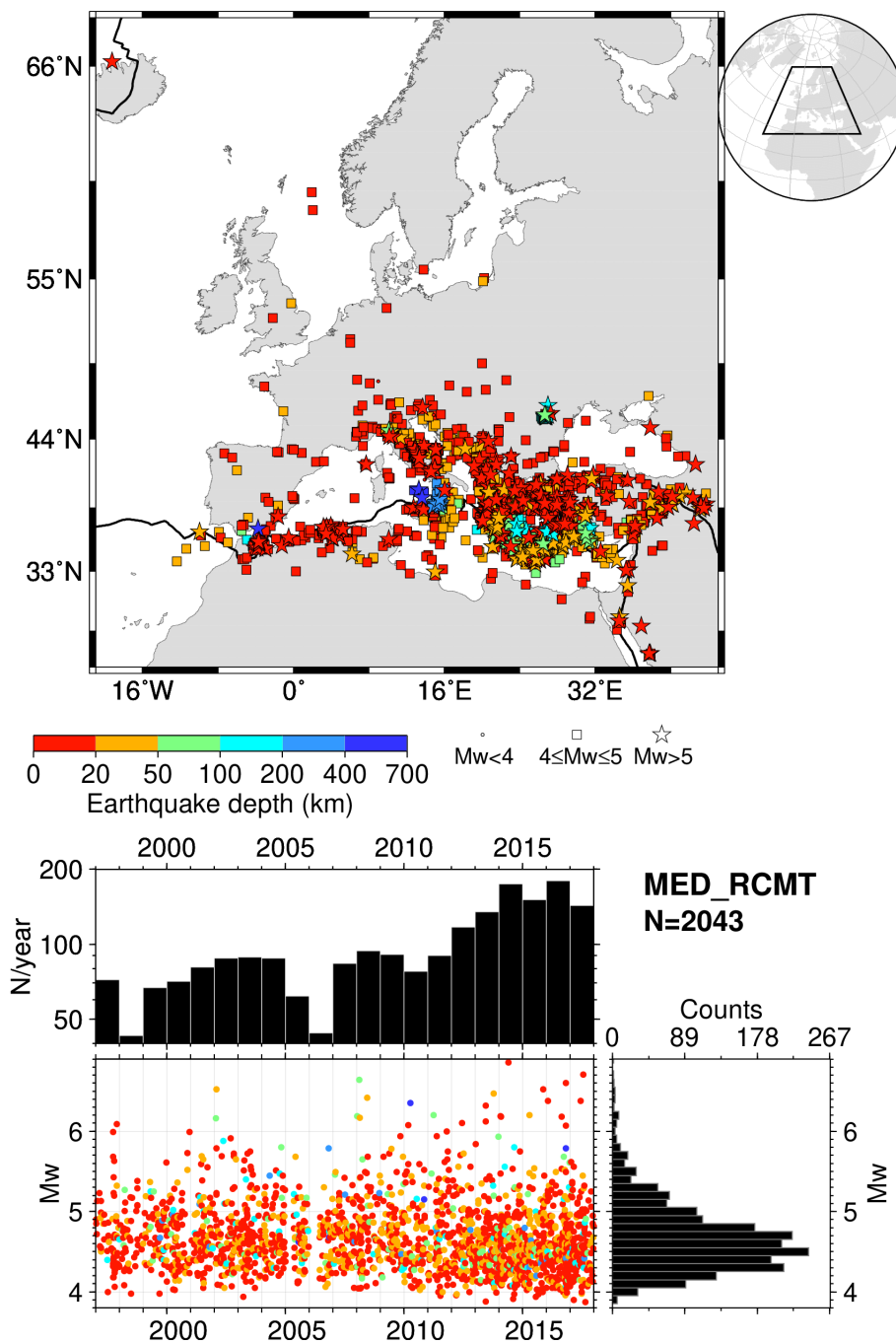
**Figure 5.** As for Fig. 2 but for agency/magnitude author = MED_RCMT. The map was drawn using the Generic Mapping Tools (GMT) (Wessel et al., 2013) software.
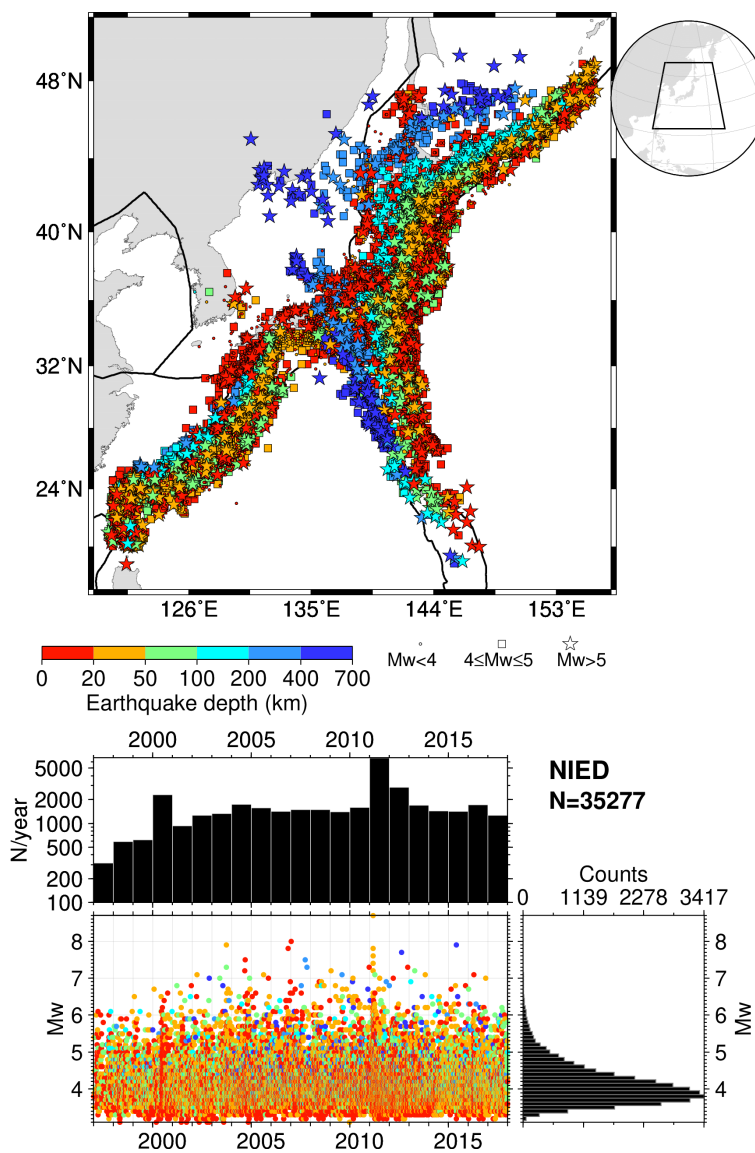
**Figure 6.** As for Fig. 2 but for agency/magnitude author = NIED. The map was drawn using the Generic Mapping Tools (GMT) (Wessel et al., 2013) software.
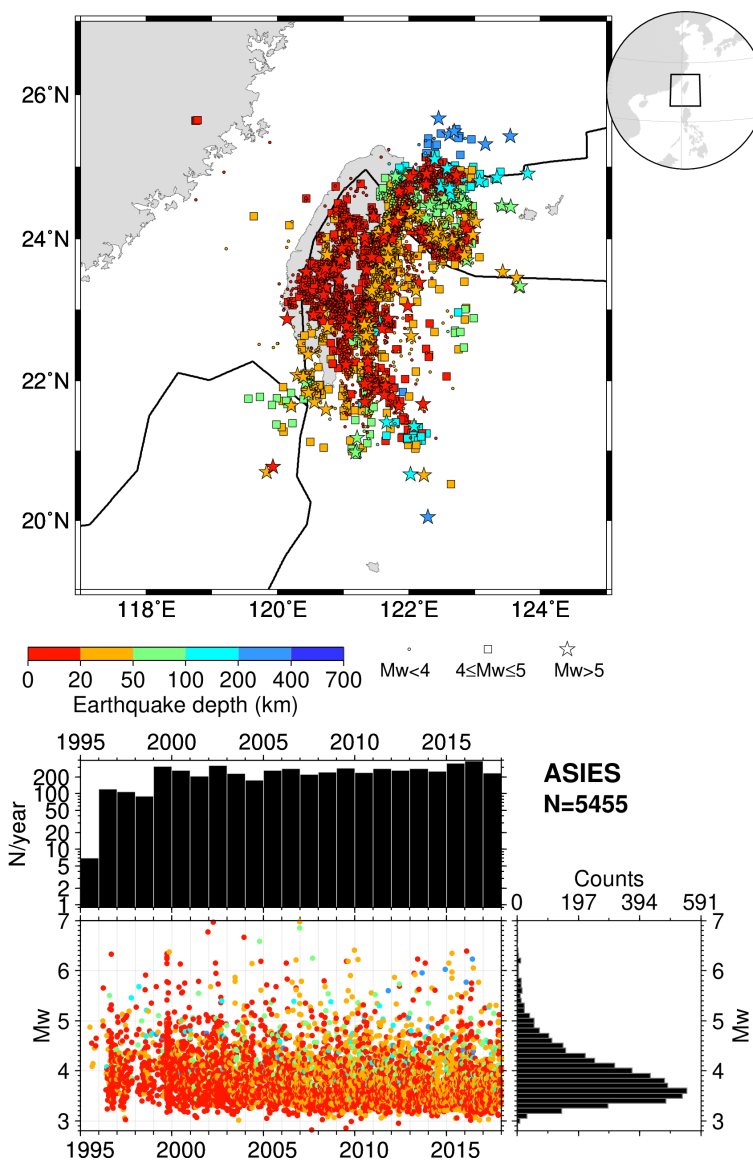
**Figure 7.** As for Fig. 2 but for agency/magnitude author = ASIES. The map was drawn using the Generic Mapping Tools (GMT) (Wessel et al., 2013) software.
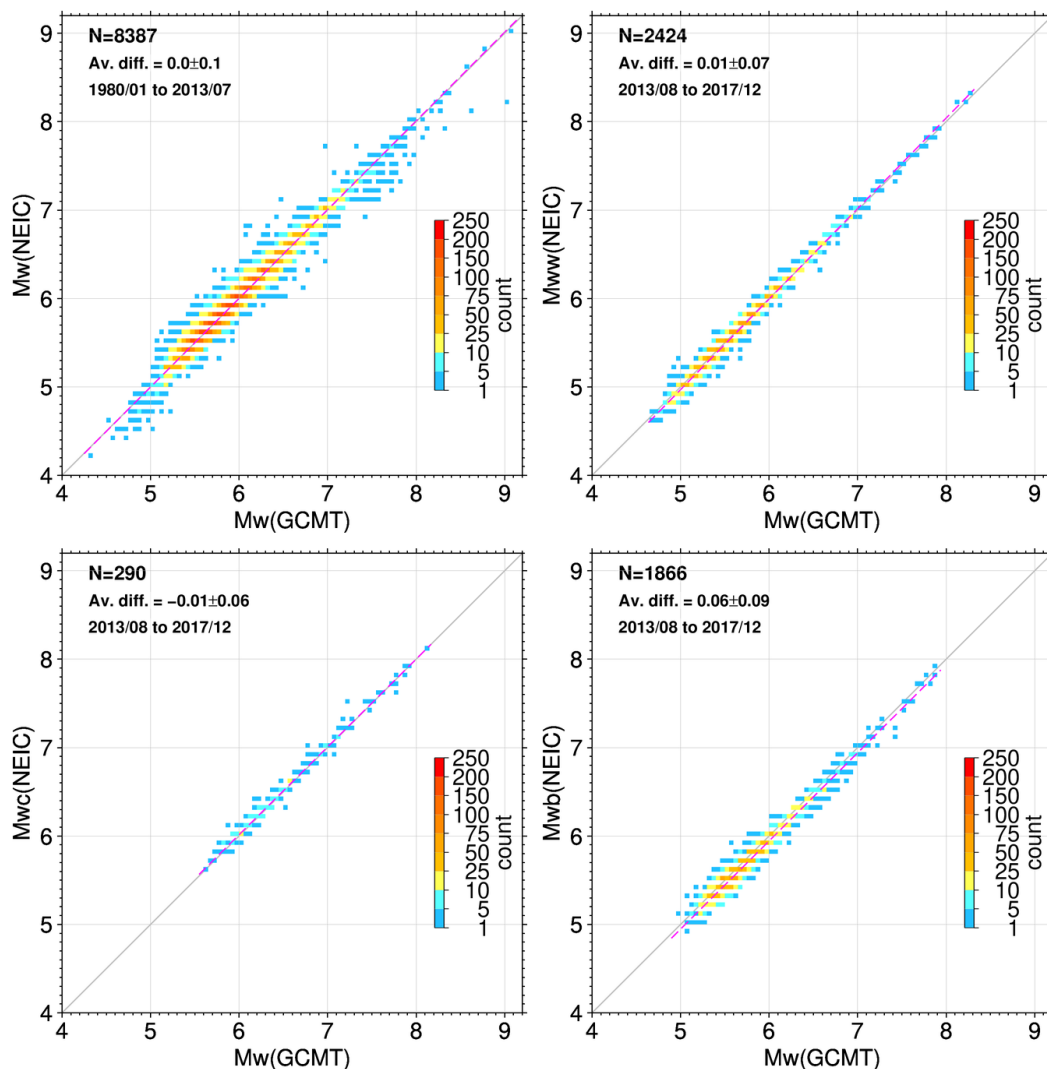
**Figure 8.** Comparison between *Mw* from GCMT and generic *Mw* NEIC for 1980-2013/07 (top left), *Mww* (top right), *Mwc* (bottom left) and *Mwb* (bottom right) for the period August 2013 - December 2017. The comparison *Mw* GCMT with *Mwr* NEIC is shown in Section 3.3.6. The distributions are shown as colour-coded data frequency for 0.1 x 0.1 m.u. cells. The magenta dashed line represents the orthogonal regression (e.g., Bormann et al., 2007; Lolli and Gasperini, 2012, and references therein). The total number of data points, average difference (*Mw* GCMT - *Mw* NEIC) and standard deviation as well as period covered are reported in top left corner of each subplot. The 1:1 lines are also shown (dashed grey lines).
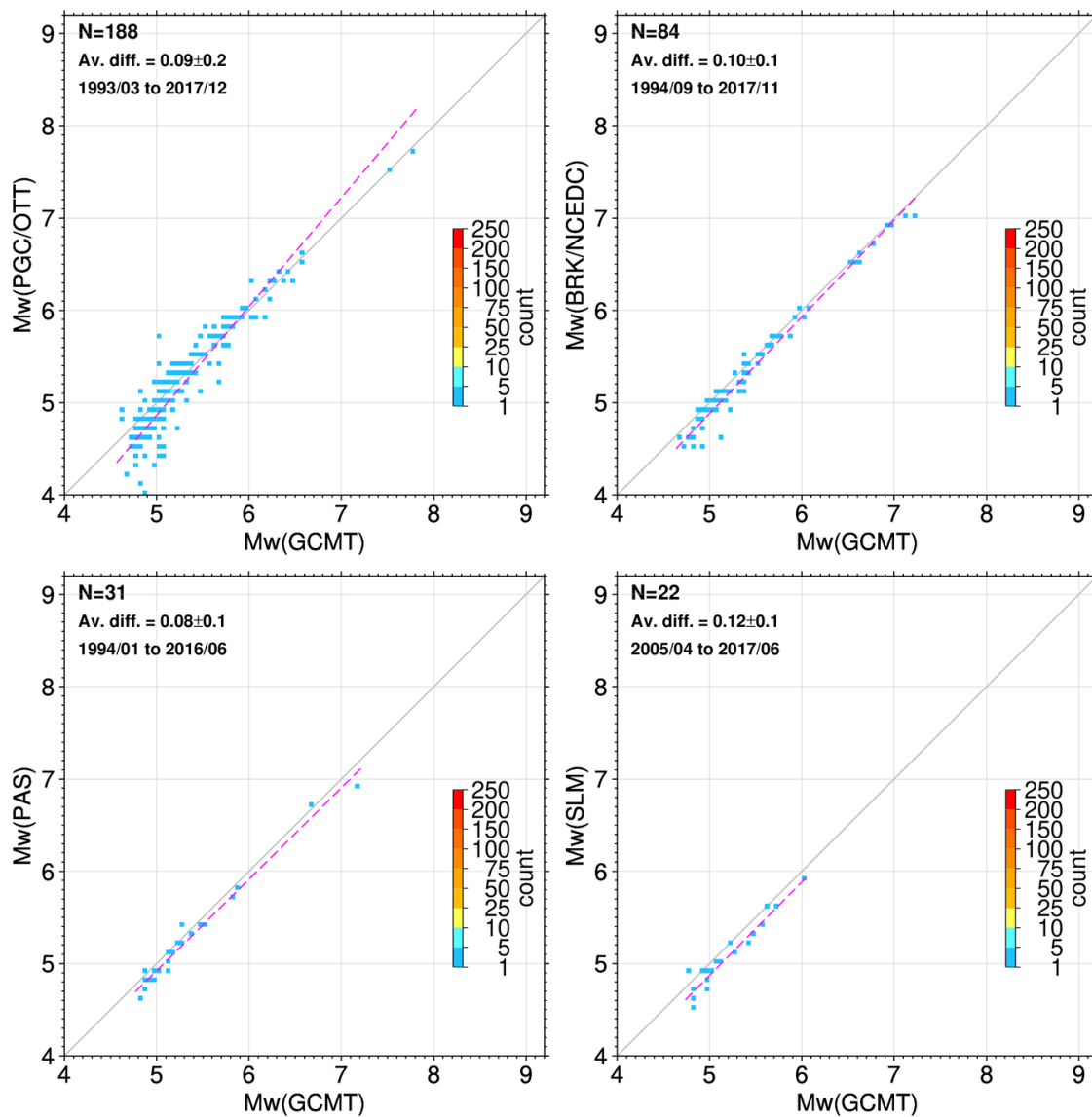
**Figure 9.** As for Fig. 8 but for GCMT and PGC/OTT (top left), GCMT and BRK/NCEDC (top right), GCMT and PAS (bottom left), GCMT and SLM (bottom right).
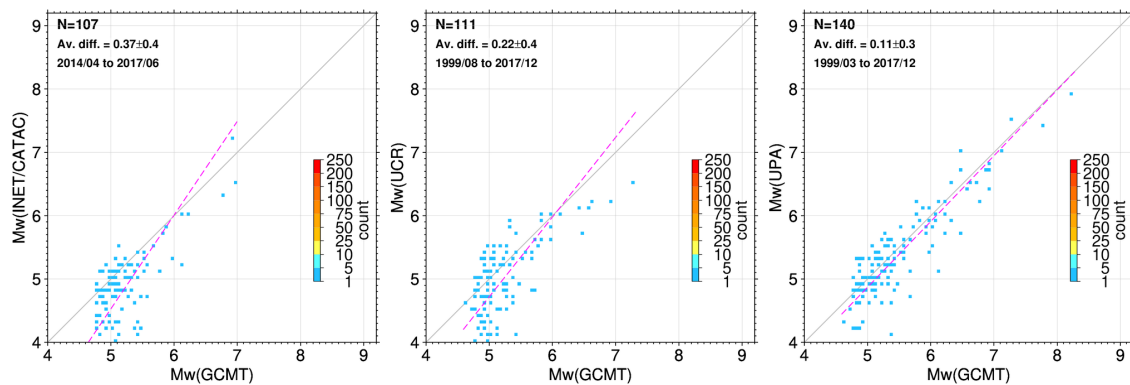
**Figure 10.** As for Fig. 8 but for GCMT and INET/CATAC (left), GCMT and UCR (middle), GCMT and UPA (right).
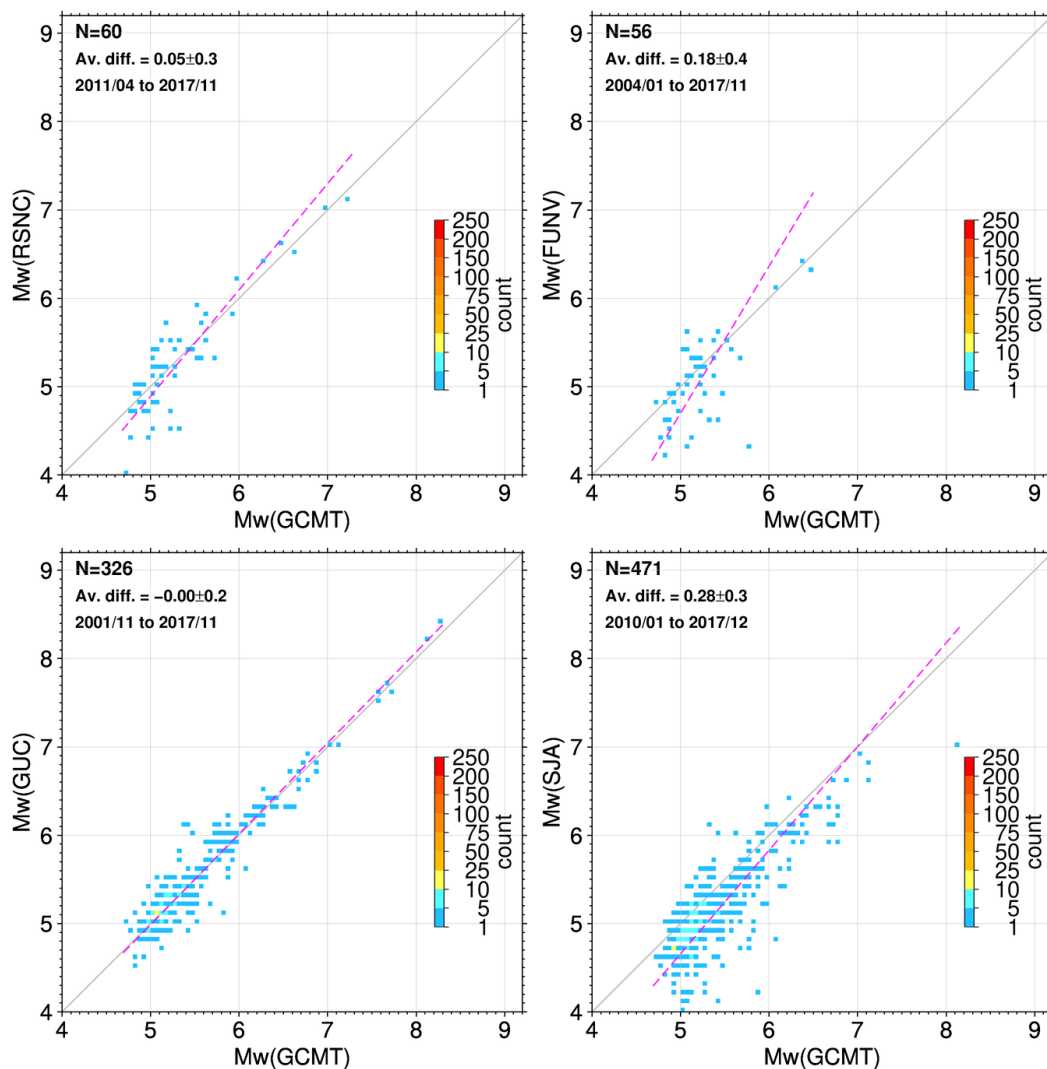
**Figure 11.** As for Fig. 8 but for GCMT and RSNC (top left), GCMT and FUNV (top right), GCMT and GUC (bottom left), GCMT and SJA (bottom right).
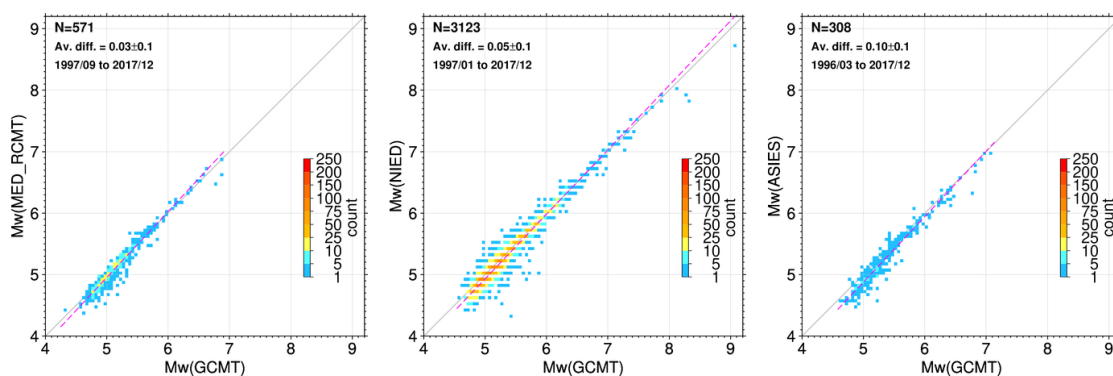
**Figure 12.** As for Fig. 8 but for GCMT and MED_RCMT (left), GCMT and NIED (middle), GCMT and ASIES (right).
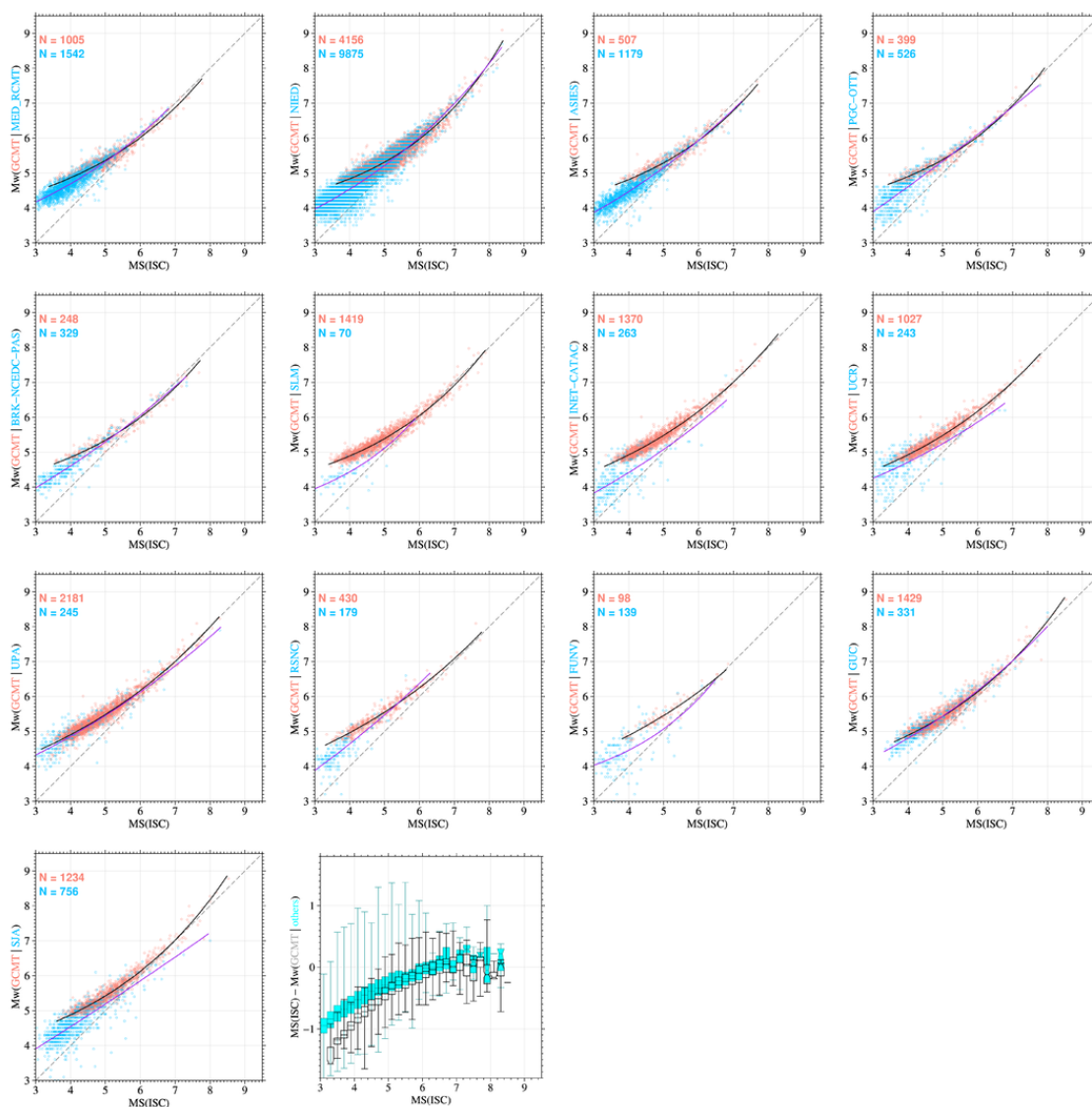
**Figure 13.** Comparisons between *MS* ISC and *Mw* GCMT (orange dots) for regional agencies (blue circles) consider in previous sections (the only difference here is that we grouped PAS with BRK/NCEDC). The nonlinear regressions between *MS* ISC and *Mw* GCMT (black solid curves) and between *MS* ISC with the regional agencies (purple solid curves) are also shown along with the 1:1 lines (dashed dark grey). The second subplot from the left at the bottom shows the box-and-whisker plot for 0.2 *MS* ISC bins of the difference between *MS* ISC and *Mw* GCMT (black, transparent) and *Mw* from all other agencies (cyan). The box represents the 25%–75% quantile, the band inside the box represents the median and the ends of the whiskers represent the minimum and maximum of all data.
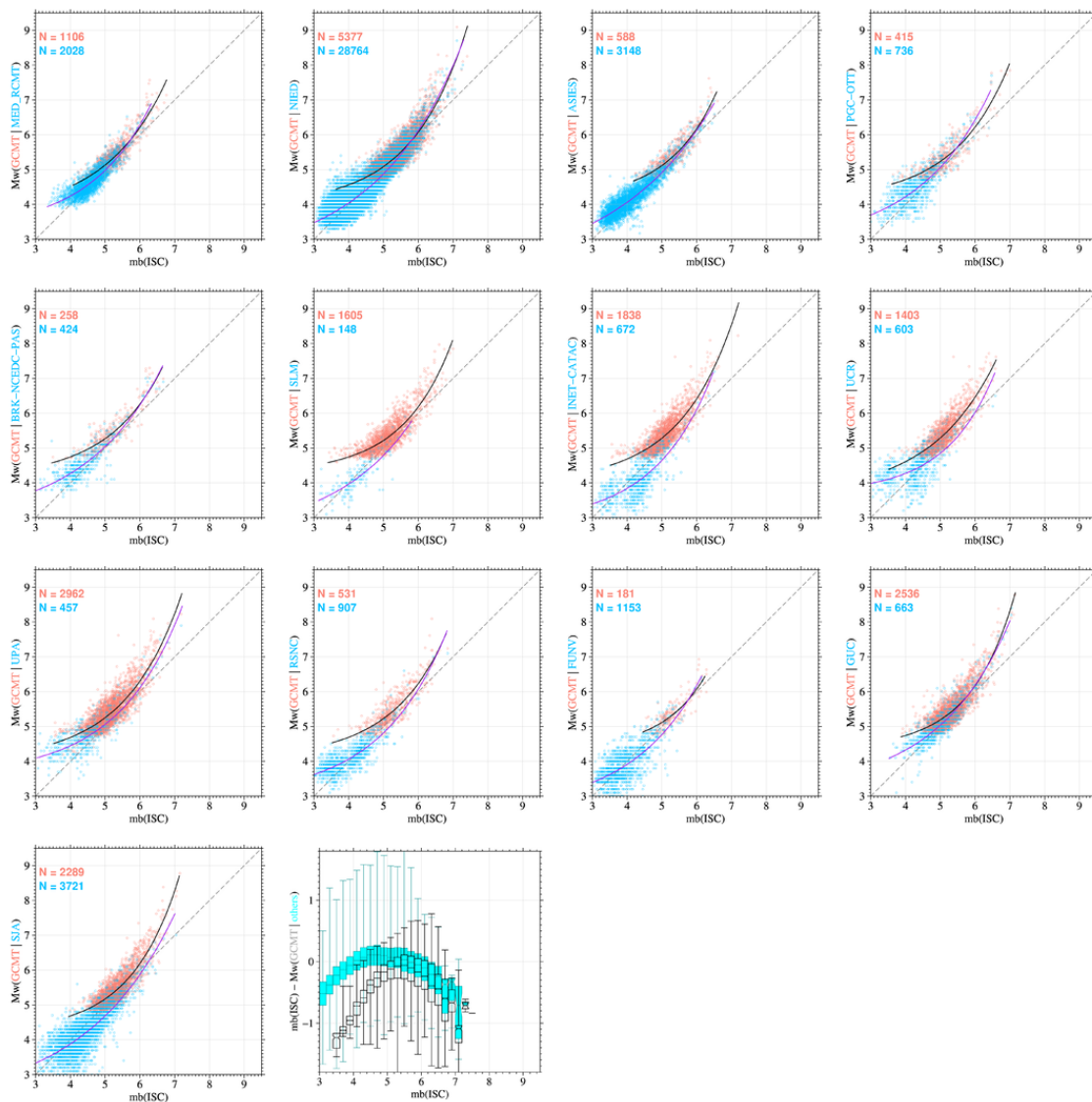
**Figure 14.** As for Fig. 13 but for *mb* ISC.
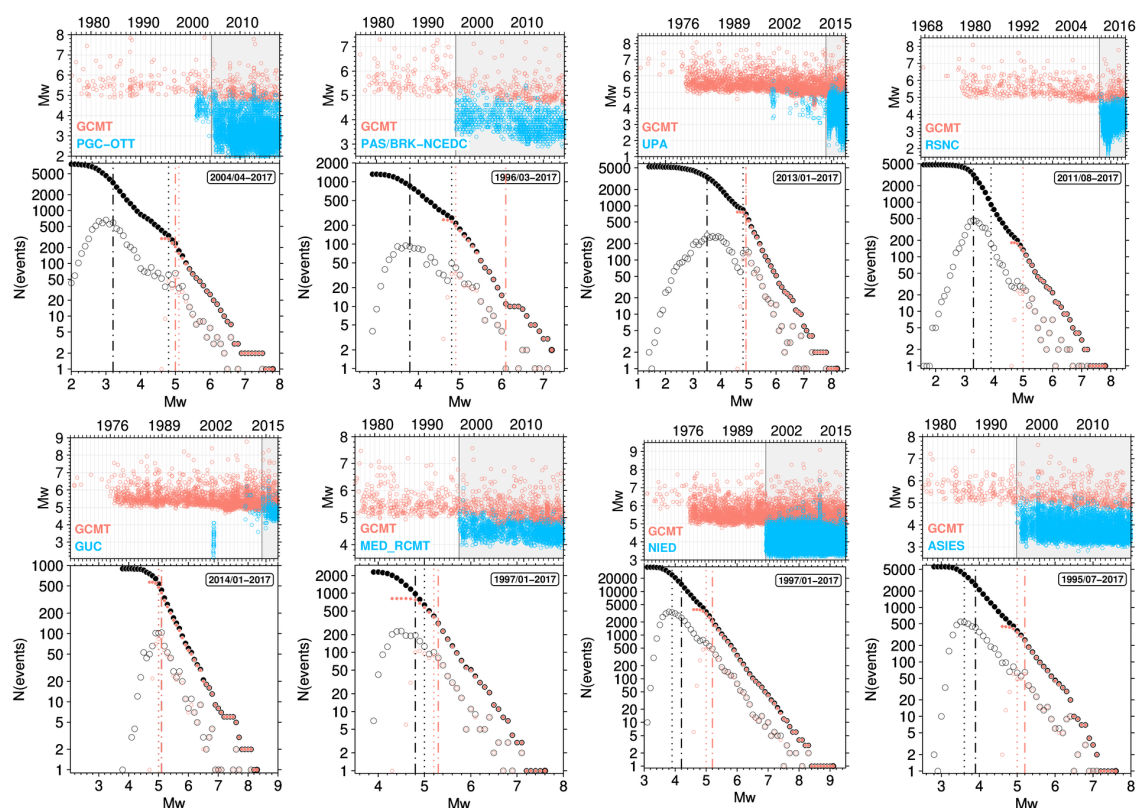
**Figure 15.** Magnitude timelines and frequency-magnitude distributions (FMD) for GCMT only (orange symbols) and GCMT complemented by some regional agency discussed above (blue in the timelines and black in the FMDs, with agency name reported in each subplot). The date range in the FMD panels (coinciding with the shaded grey areas in the timeline panels) in every subplot identifies the time period over which the FMD have been obtained both for GCMT alone and by complementing it with the corresponding regional agency. The filled and empty circles are cumulative and single frequencies, respectively. The dashed-dotted vertical lines (orange for GCMT only, black for GCMT and regional agency) depict the magnitude of completeness (Mc) obtained with the median-based analysis of the segment slope by Amorese (2007), whereas the dotted vertical lines depict the Mc as obtained from the goodness-of-fit test by Wiemer and Wyss (2000). Note that Mc values for Chile (as covered by agency GUC) are identical for GCMT and GCMT + GUC, as from the timeline the GUC contribution started only in recent years. All the Mc values shown here have been obtained by using the rseismNet R package by A. Mignan, available at https://github.com/amignan/rseismNet, last accessed in September 2020. Details about the Mc estimation methods can be found in Mignan and Woessner (2012).
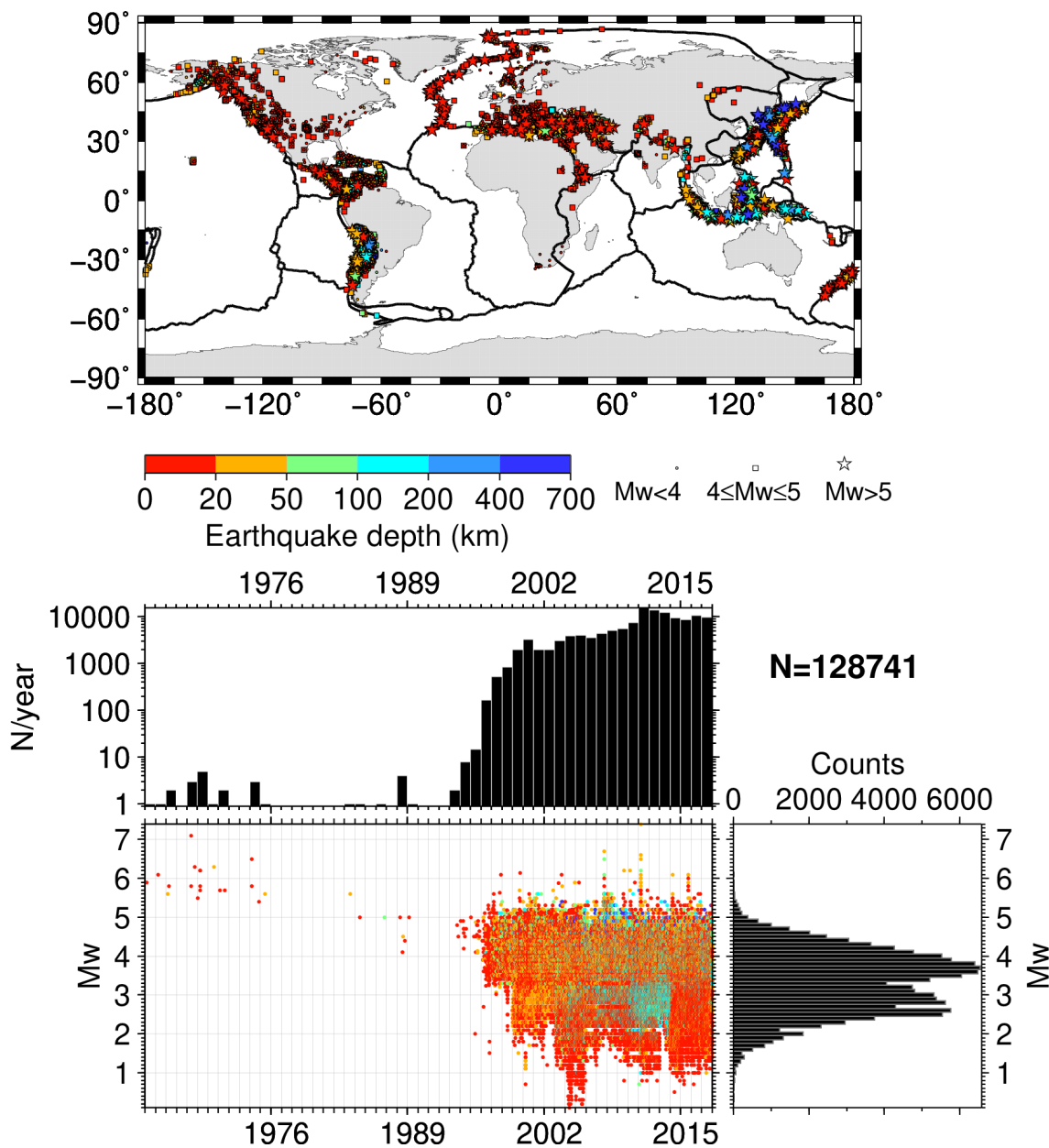
**Figure 16.** As for Fig. 2 but for earthquakes with *Mw* from regional agencies only (i.e., earthquakes with *Mw* from global agencies, with the exception of *Mwr* from NEIC, are excluded). The map was drawn using the Generic Mapping Tools (GMT) (Wessel et al., 2013) software.

**Appendix A: Additional plots**

550 Here we include additional summary plots similar to Fig. 2 or magnitude comparisons similar to Fig. 8 for agencies/magnitude authors or specific types of $Mw$ that were not discussed in detail in the main text.
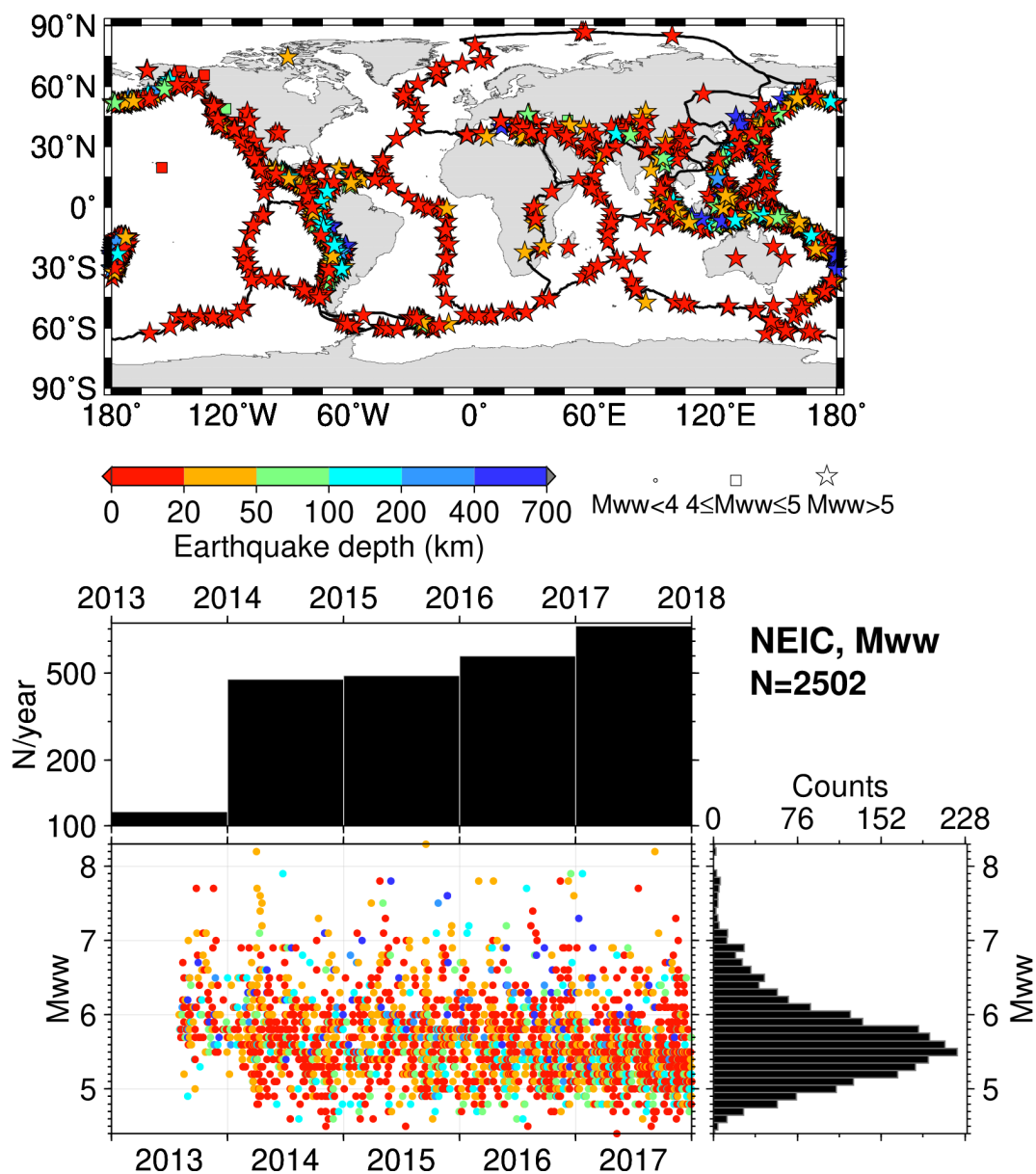
**Figure A1.** As for Fig. 2 but for agency/magnitude author = NEIC and *Mww*. The map was drawn using the Generic Mapping Tools (GMT) (Wessel et al., 2013) software.
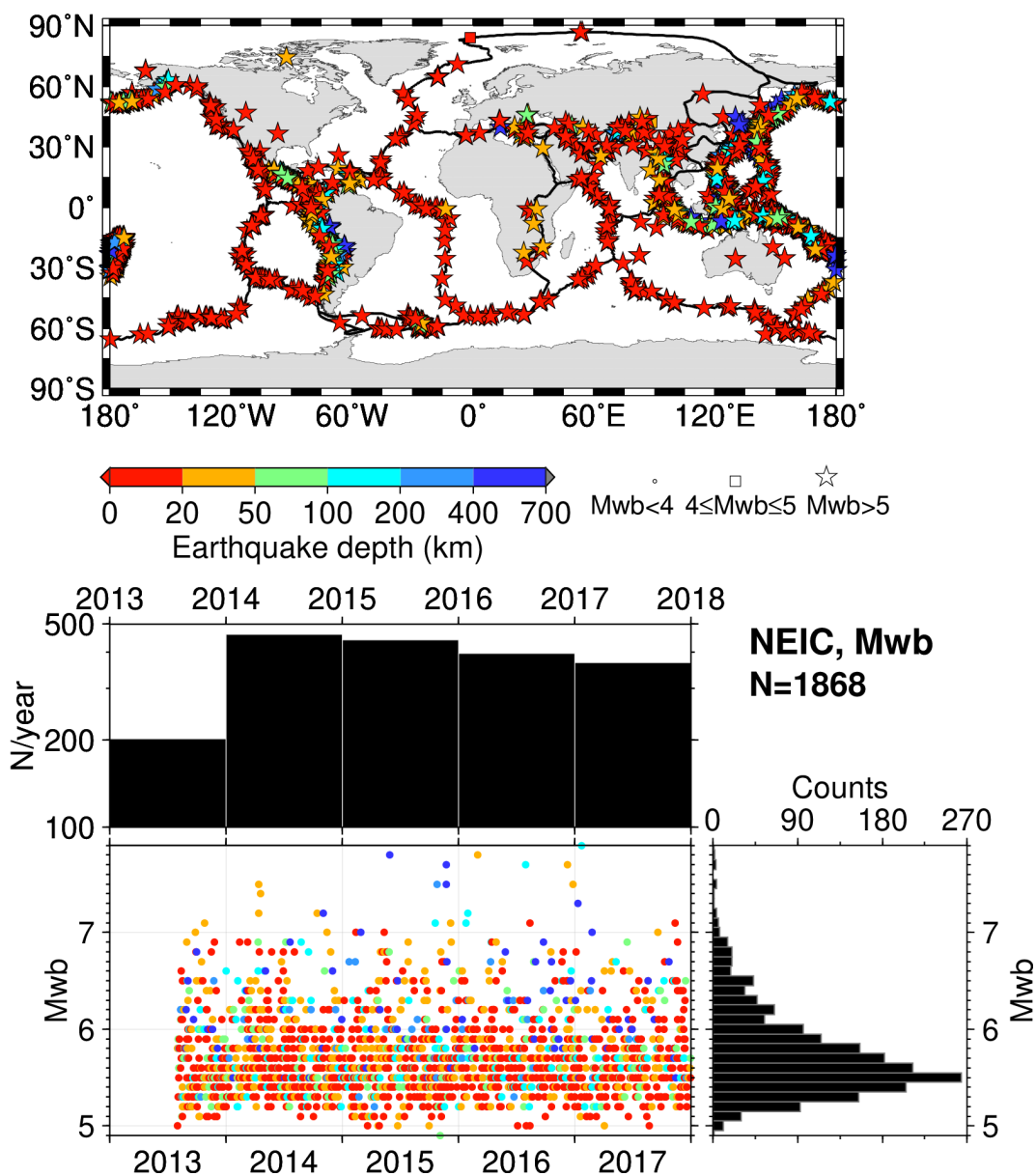
**Figure A2.** As for Fig. 2 but for agency/magnitude author = NEIC and *Mwb*. The map was drawn using the Generic Mapping Tools (GMT) (Wessel et al., 2013) software.
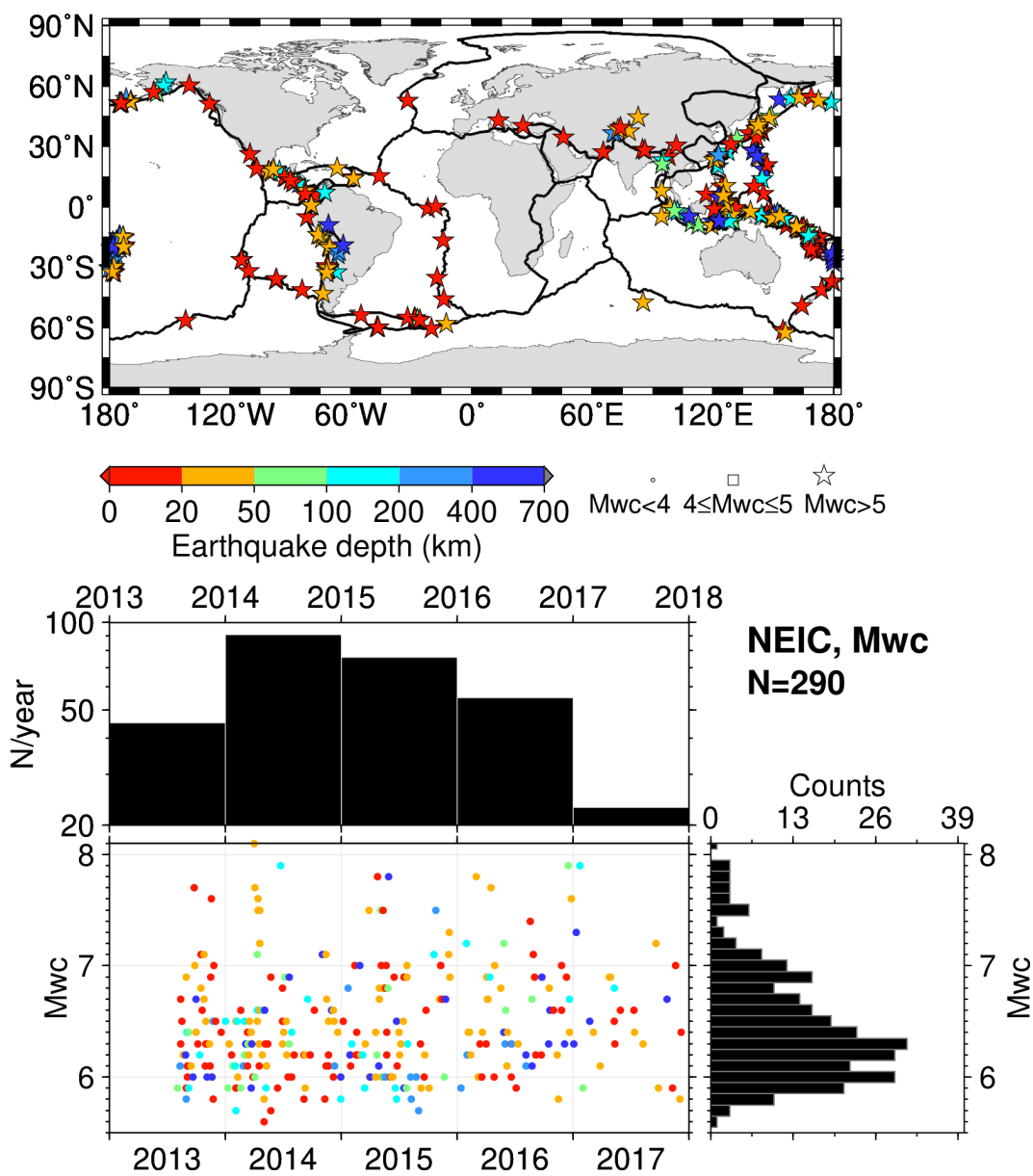
**Figure A3.** As for Fig. 2 but for agency/magnitude author = NEIC and *Mwc*. The map was drawn using the Generic Mapping Tools (GMT) (Wessel et al., 2013) software.
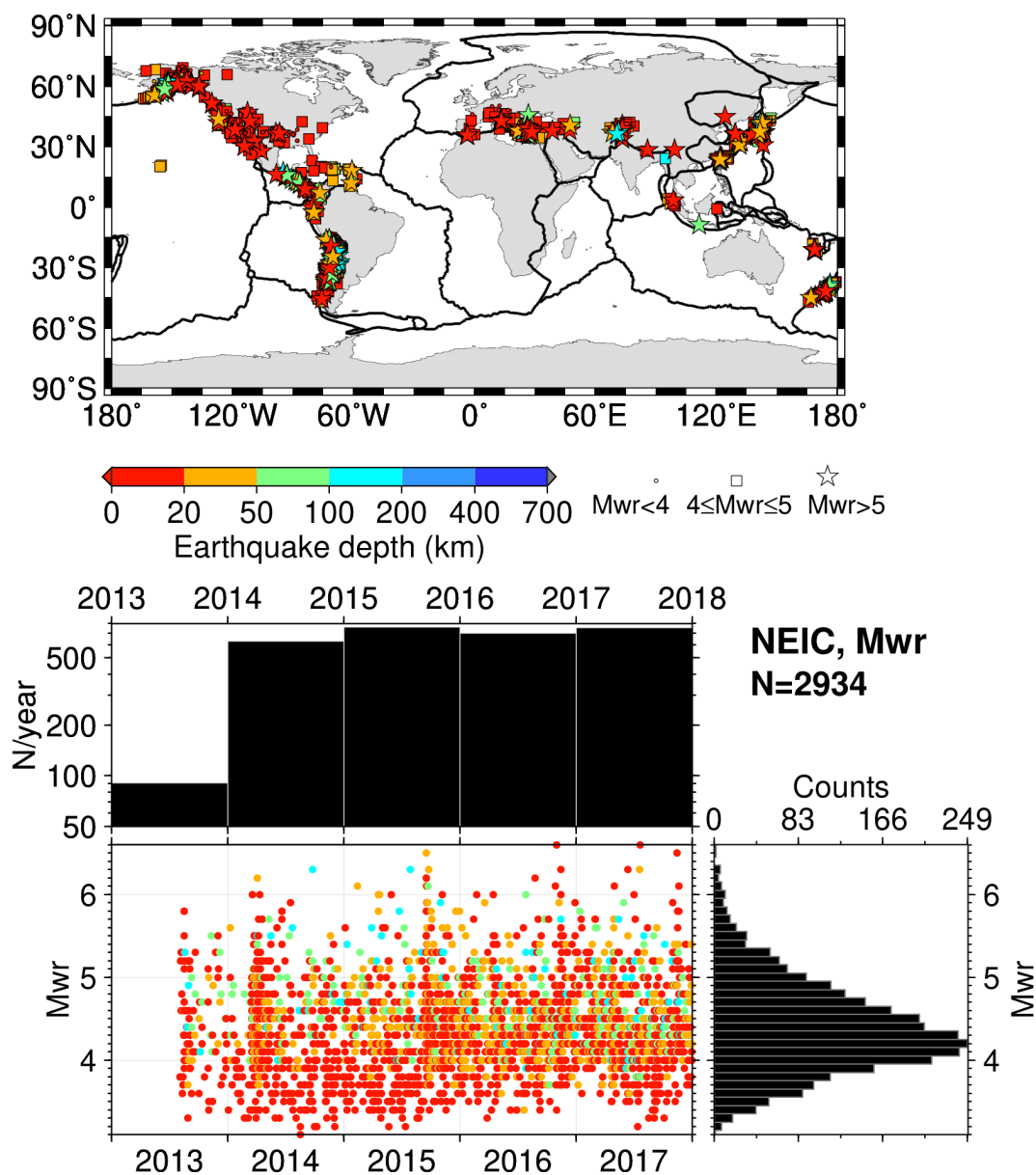
**Figure A4.** As for Fig. 2 but for agency/magnitude author = NEIC and *Mwr*. The map was drawn using the Generic Mapping Tools (GMT) (Wessel et al., 2013) software.
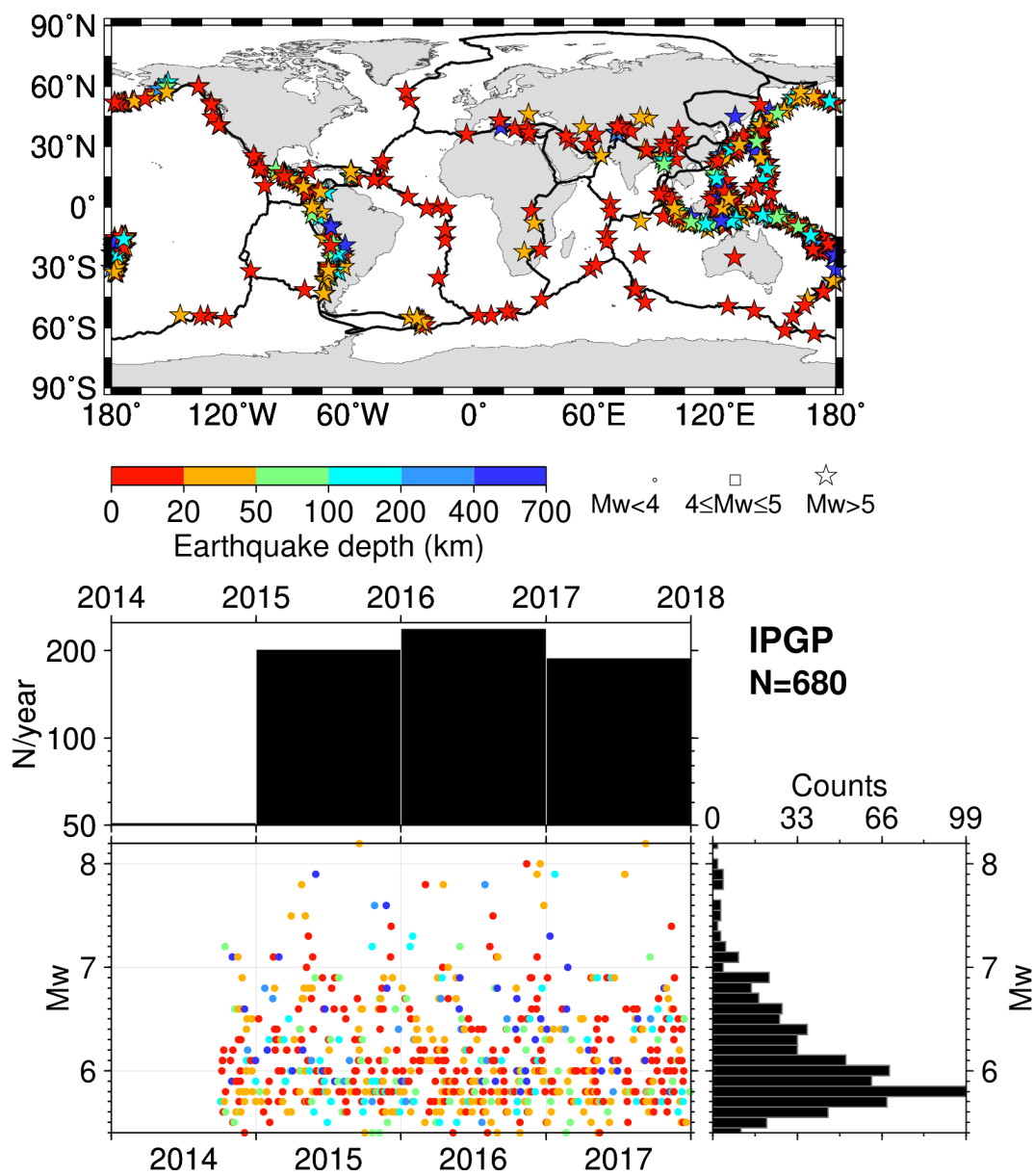
**Figure A5.** As for Fig. 2 but for agency/magnitude author = IPGP. The map was drawn using the Generic Mapping Tools (GMT) (Wessel et al., 2013) software.
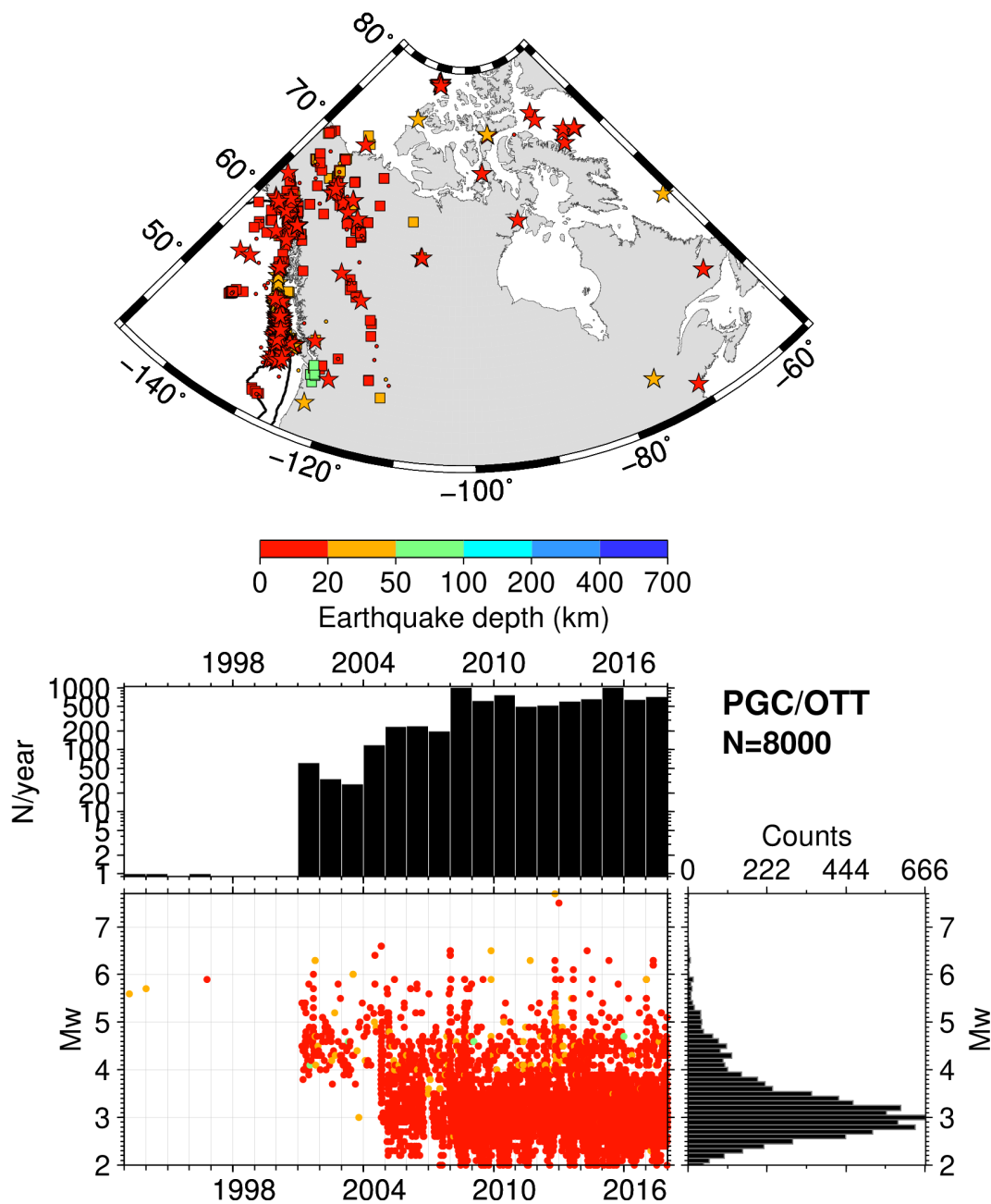
**Figure A6.** As for Fig. 2 but for agency/magnitude author = PGC and OTT. The procedures used by this reporter are described at http://www.isc.ac.uk/iscbulletin/agencies/OTT-MW-mags.pdf and Mulder (2015). The map was drawn using the Generic Mapping Tools (GMT) (Wessel et al., 2013) software.
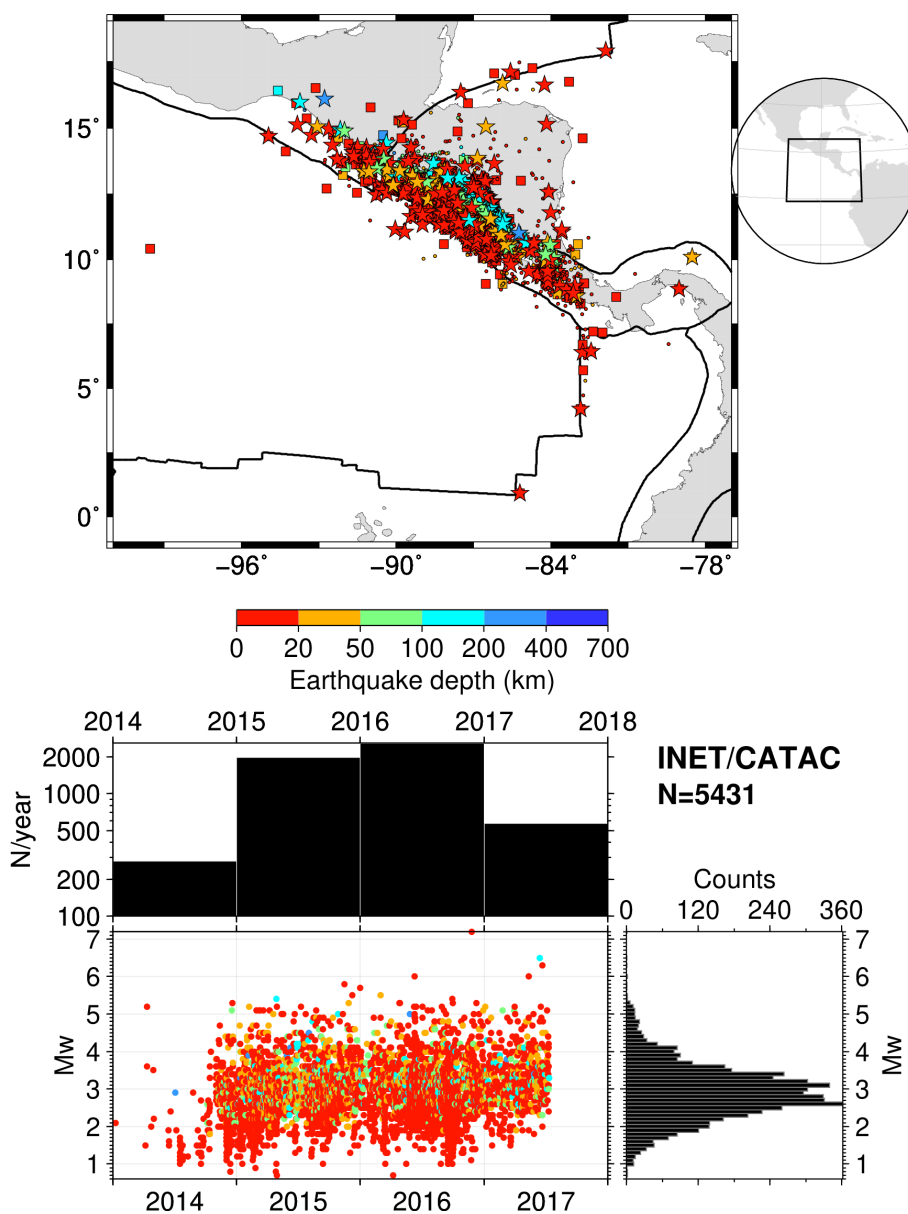
**Figure A7.** As for Fig. 2 but for agency/magnitude author = INET and CATAC. The map was drawn using the Generic Mapping Tools (GMT) (Wessel et al., 2013) software.
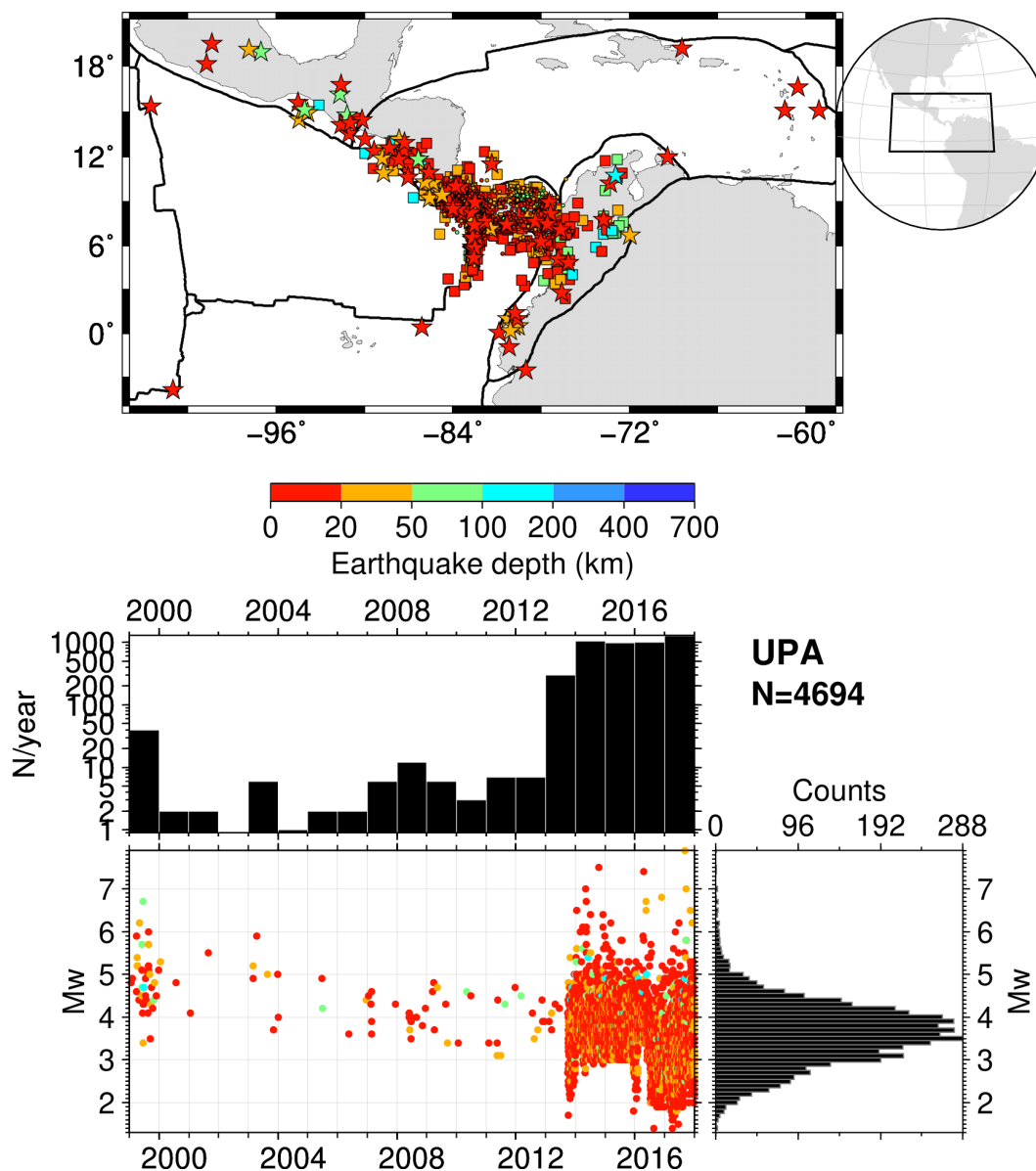
**Figure A8.** As for Fig. 2 but for agency/magnitude author = UPA. The map was drawn using the Generic Mapping Tools (GMT) (Wessel et al., 2013) software.
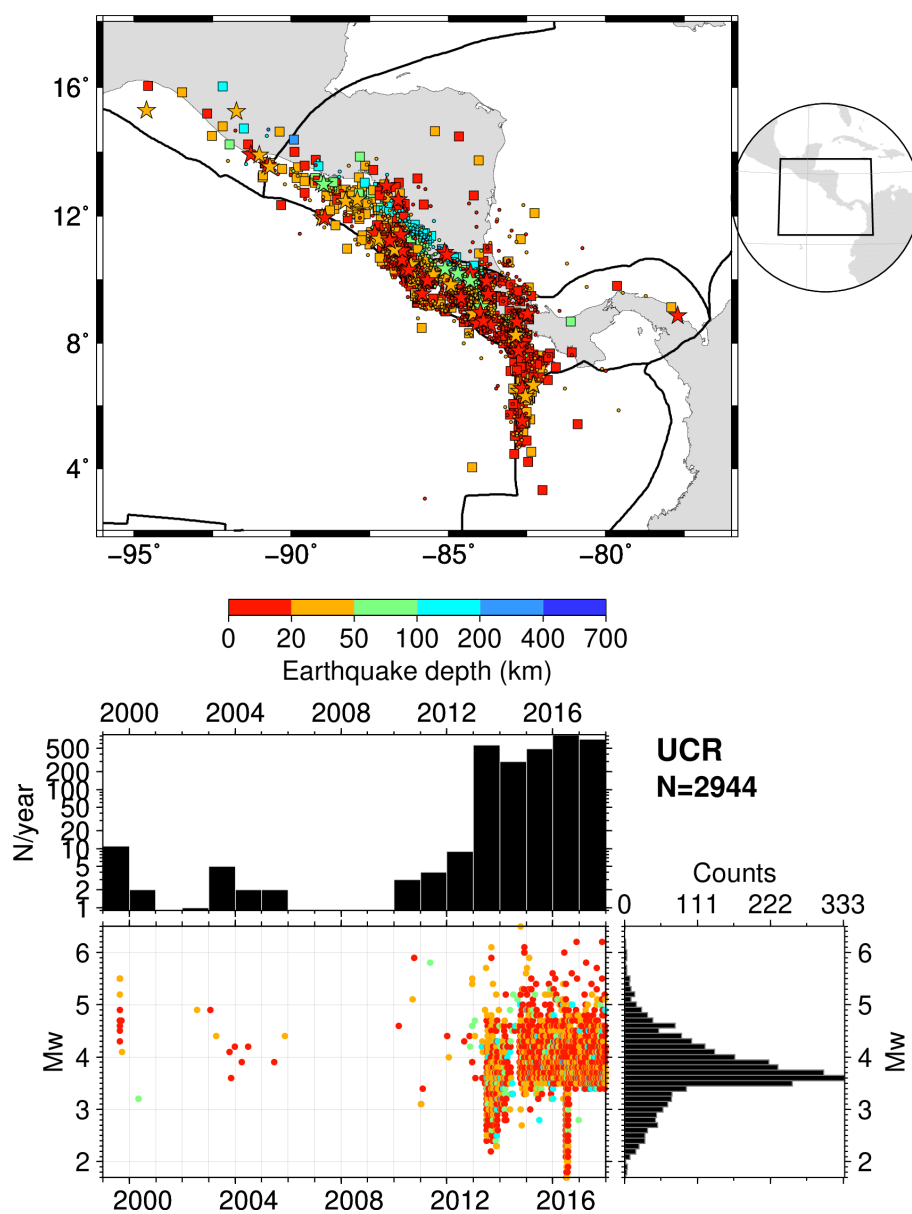
**Figure A9.** As for Fig. 2 but for agency/magnitude author = UCR. The map was drawn using the Generic Mapping Tools (GMT) (Wessel et al., 2013) software.
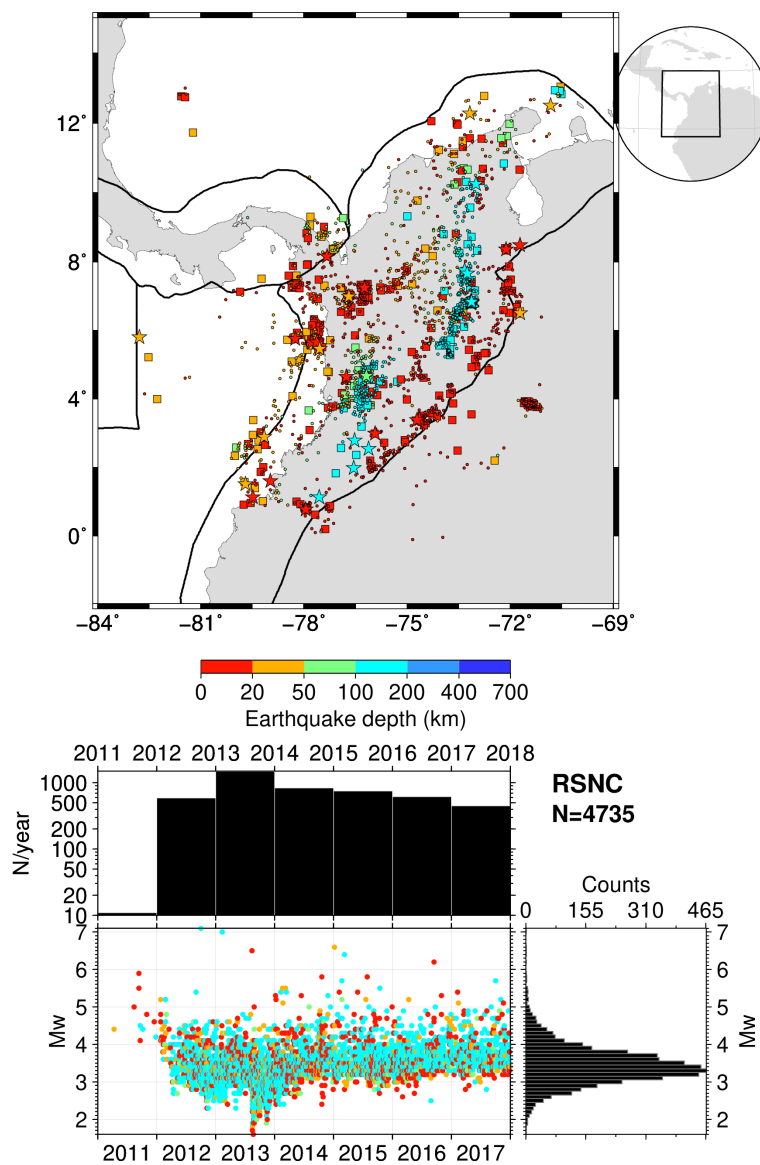
**Figure A10.** As for Fig. 2 but for agency/magnitude author = RSNC. The map was drawn using the Generic Mapping Tools (GMT) (Wessel et al., 2013) software.
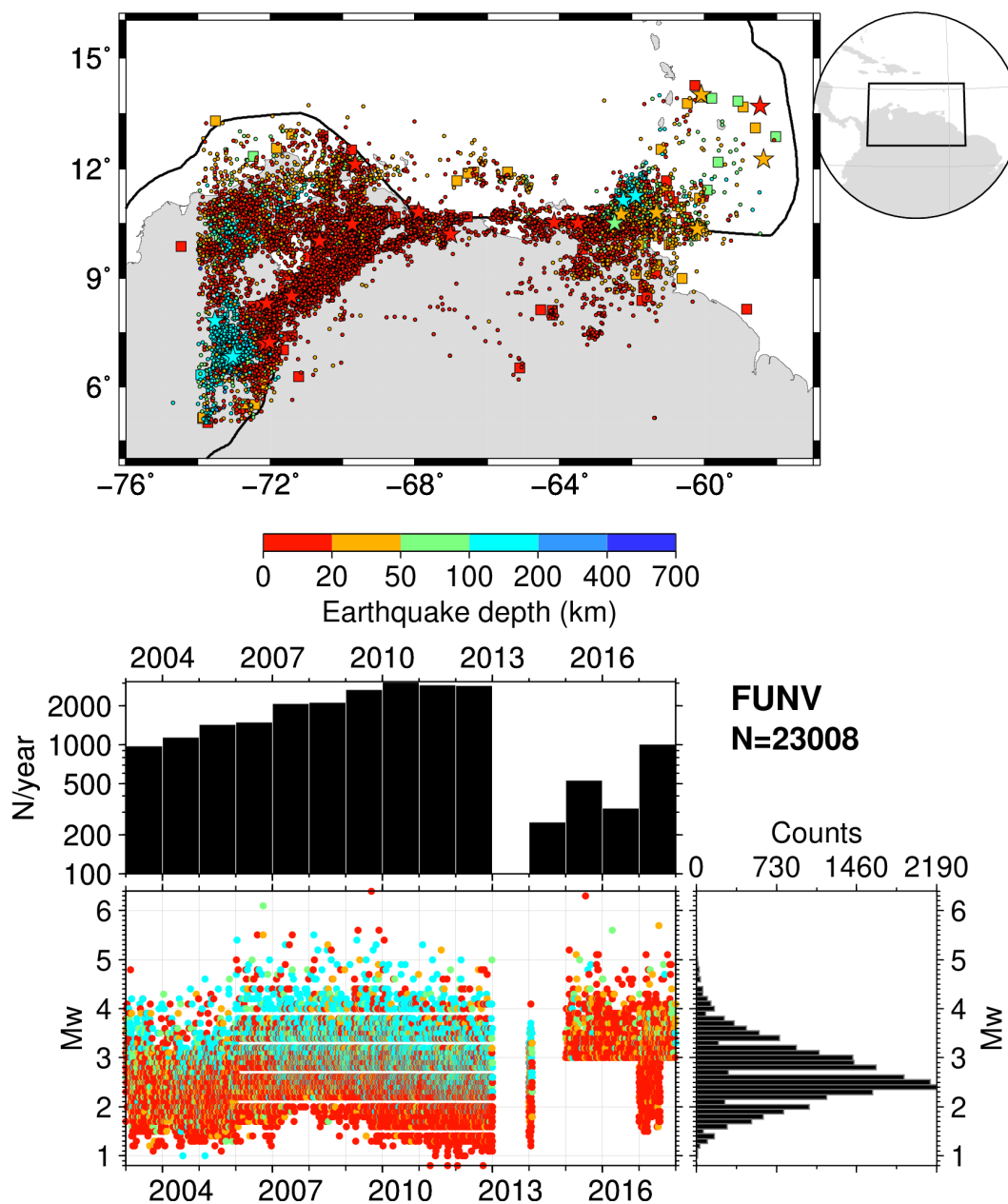
**Figure A11.** As for Fig. 2 but for agency/magnitude author = FUNV. Possible rounding effects in pre-2013 *Mw* values are visible in the timeline and histograms. The map was drawn using the Generic Mapping Tools (GMT) (Wessel et al., 2013) software.
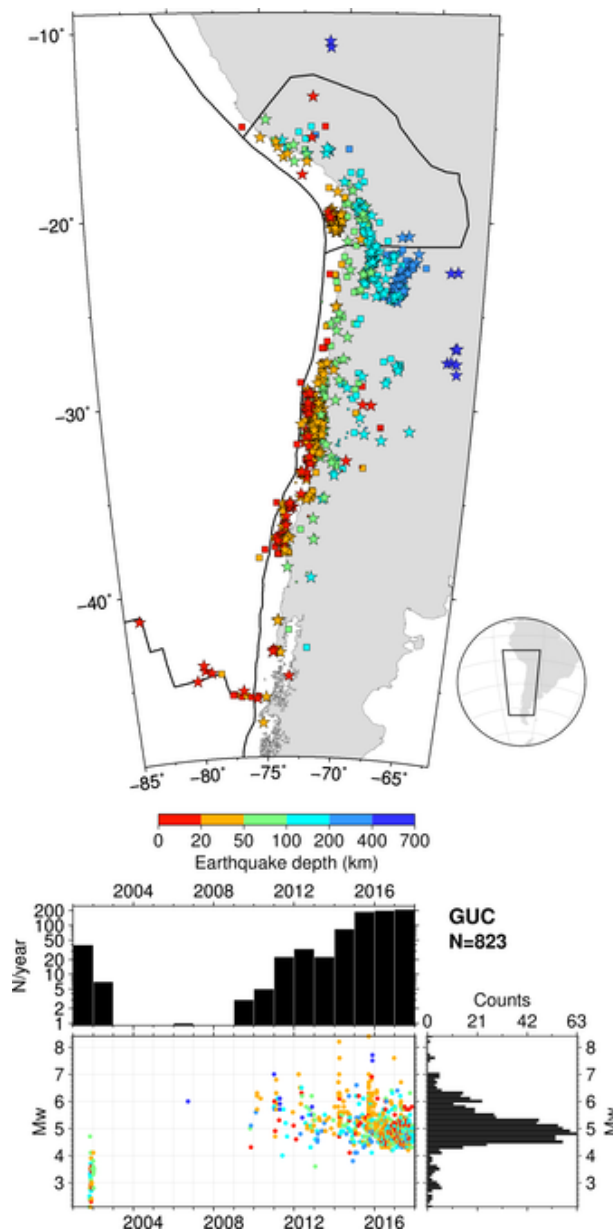
**Figure A12.** As for Fig. 2 but for agency/magnitude author = GUC. The map was drawn using the Generic Mapping Tools (GMT) (Wessel et al., 2013) software.
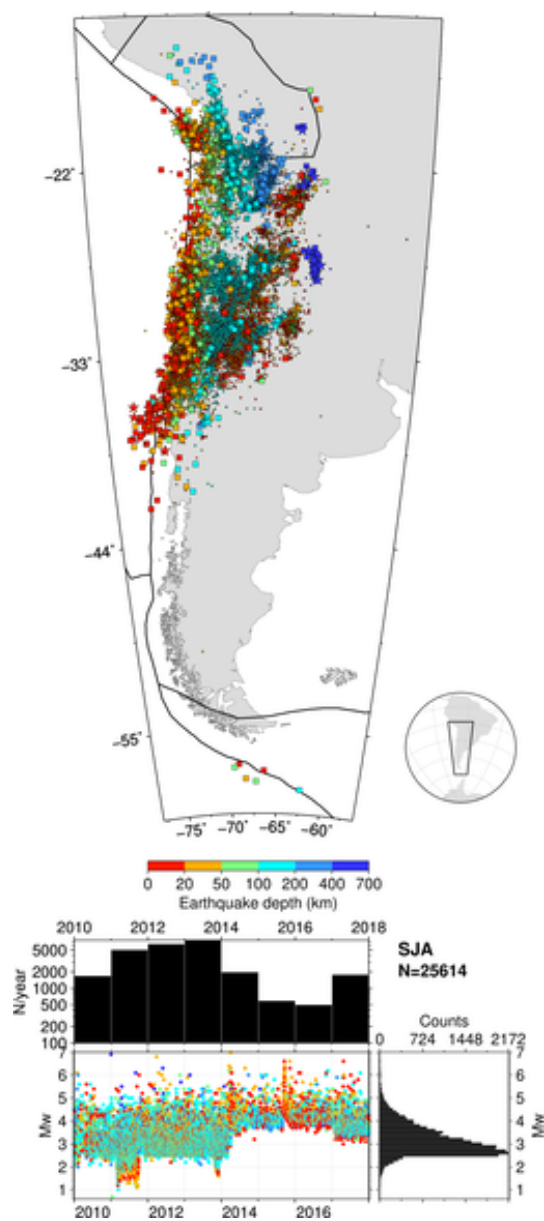
**Figure A13.** As for Fig. 2 but for agency/magnitude author = SJA. The map was drawn using the Generic Mapping Tools (GMT) (Wessel et al., 2013) software.
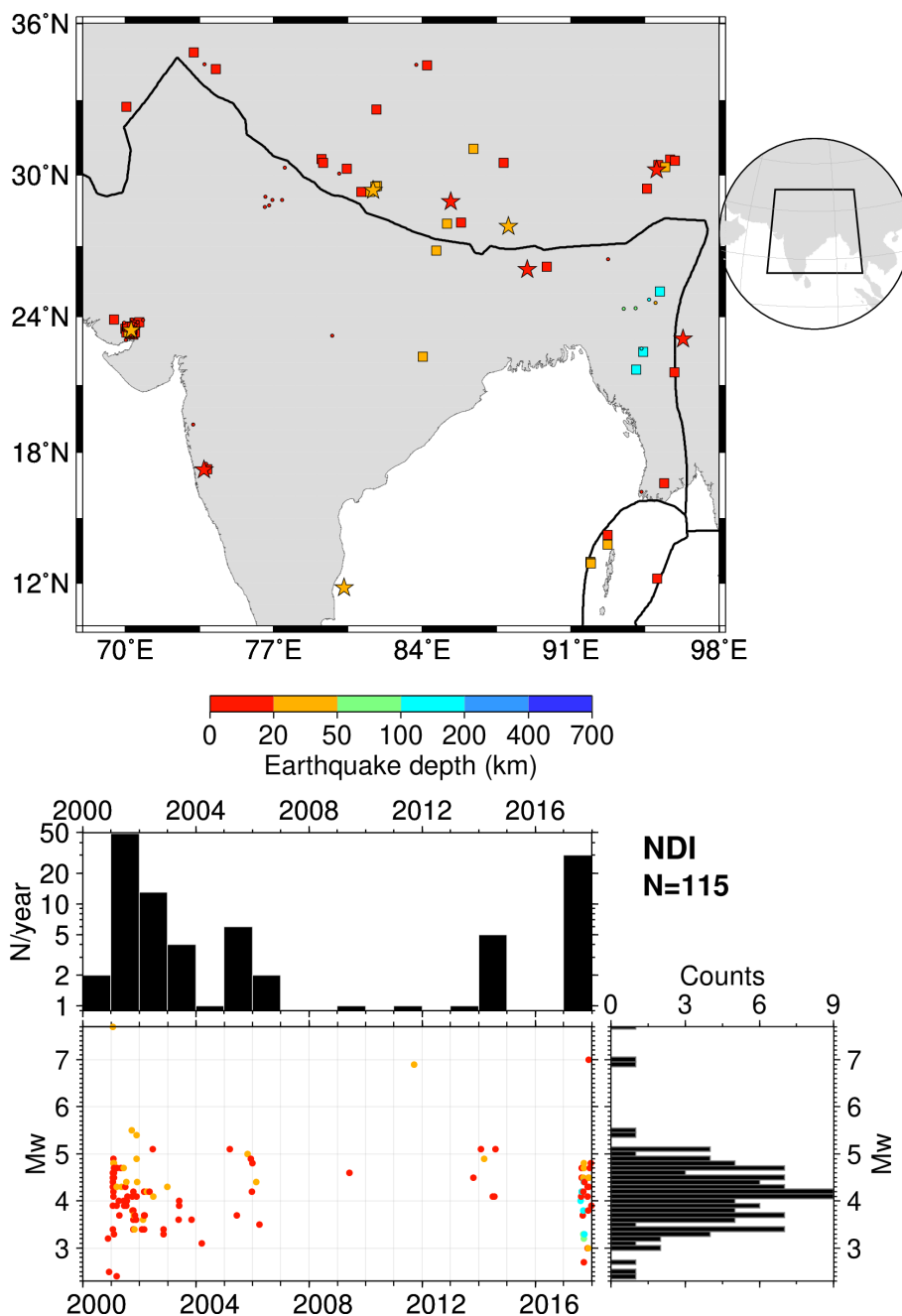
**Figure A14.** As for Fig. 2 but for agency/magnitude author = NDI. The map was drawn using the Generic Mapping Tools (GMT) (Wessel et al., 2013) software.
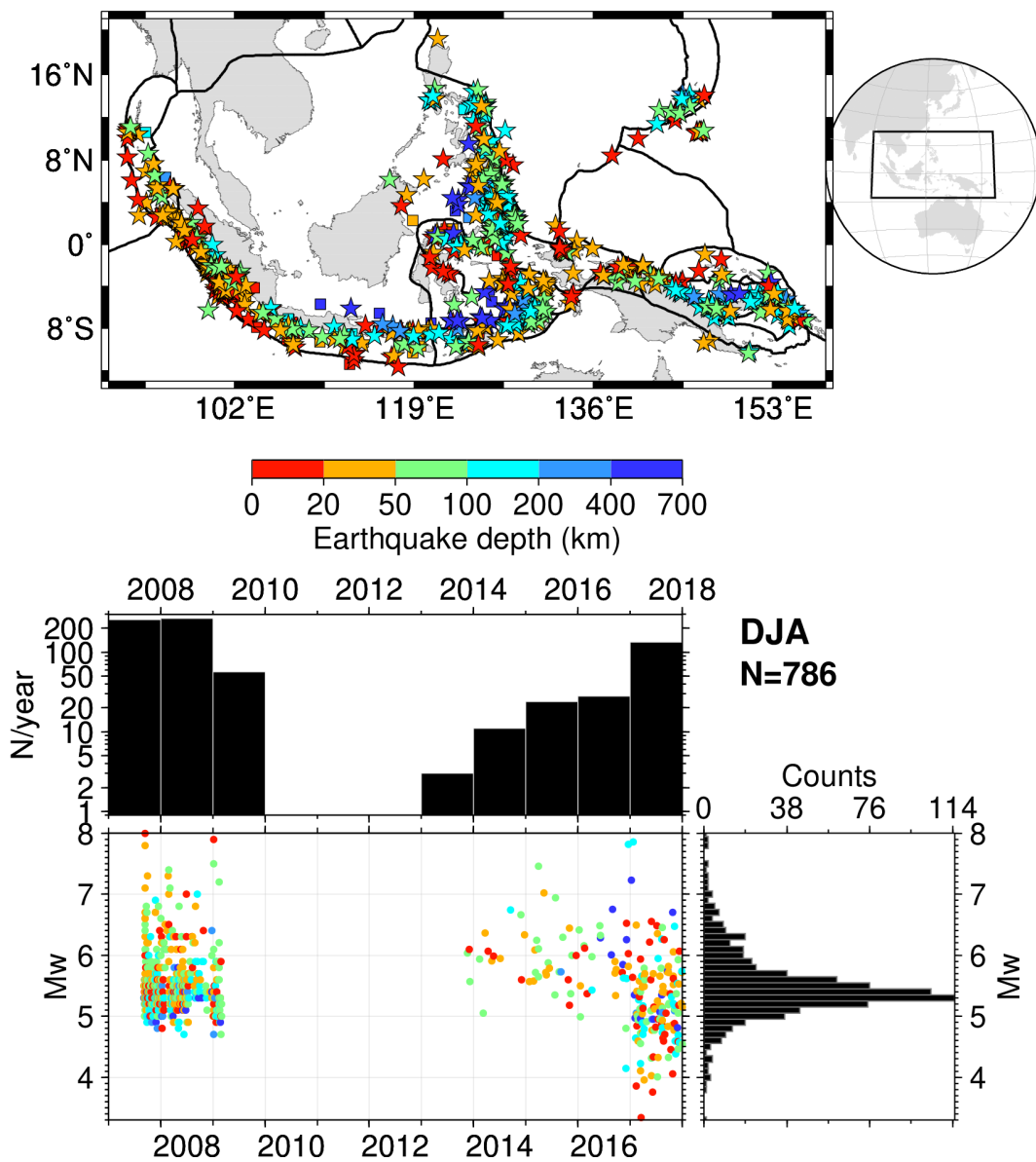
**Figure A15.** As for Fig. 2 but for agency/magnitude author = DJA. The map was drawn using the Generic Mapping Tools (GMT) (Wessel et al., 2013) software.
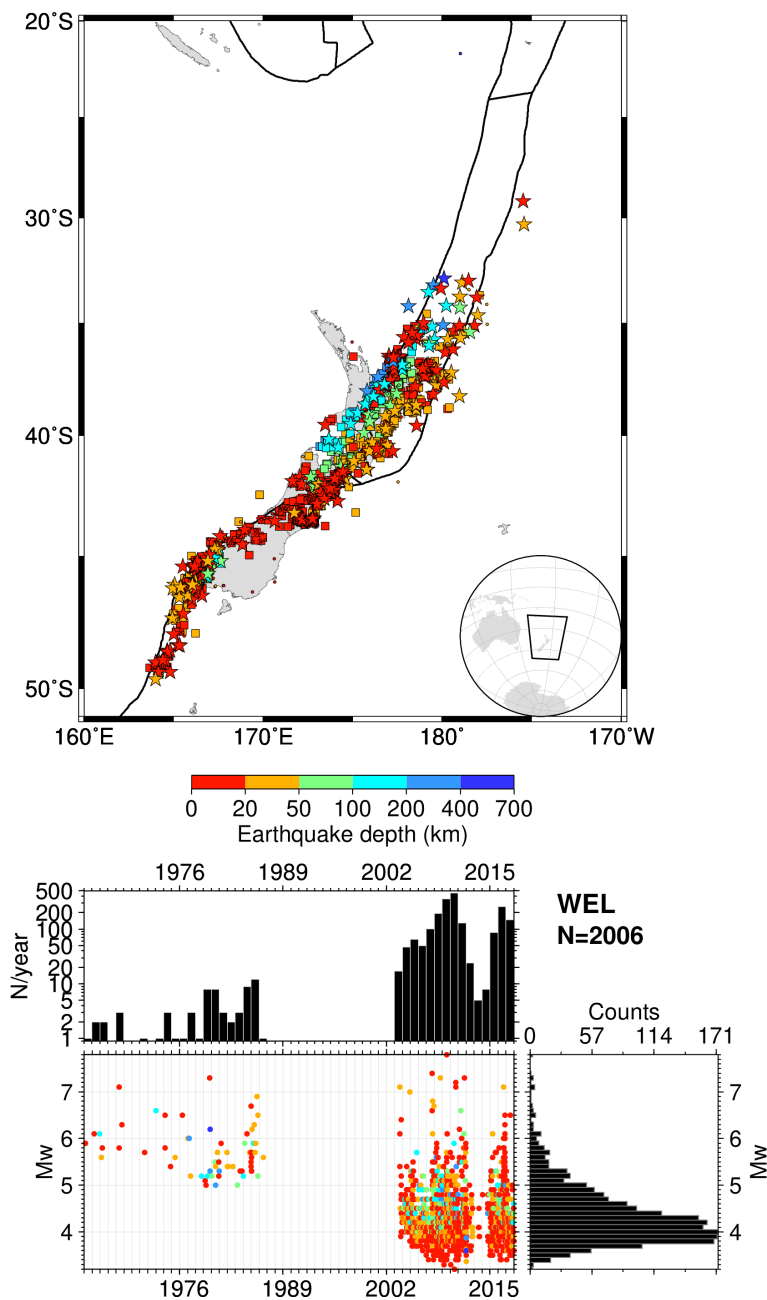
**Figure A16.** As for Fig. 2 but for agency/magnitude author = WEL. The map was drawn using the Generic Mapping Tools (GMT) (Wessel et al., 2013) software.
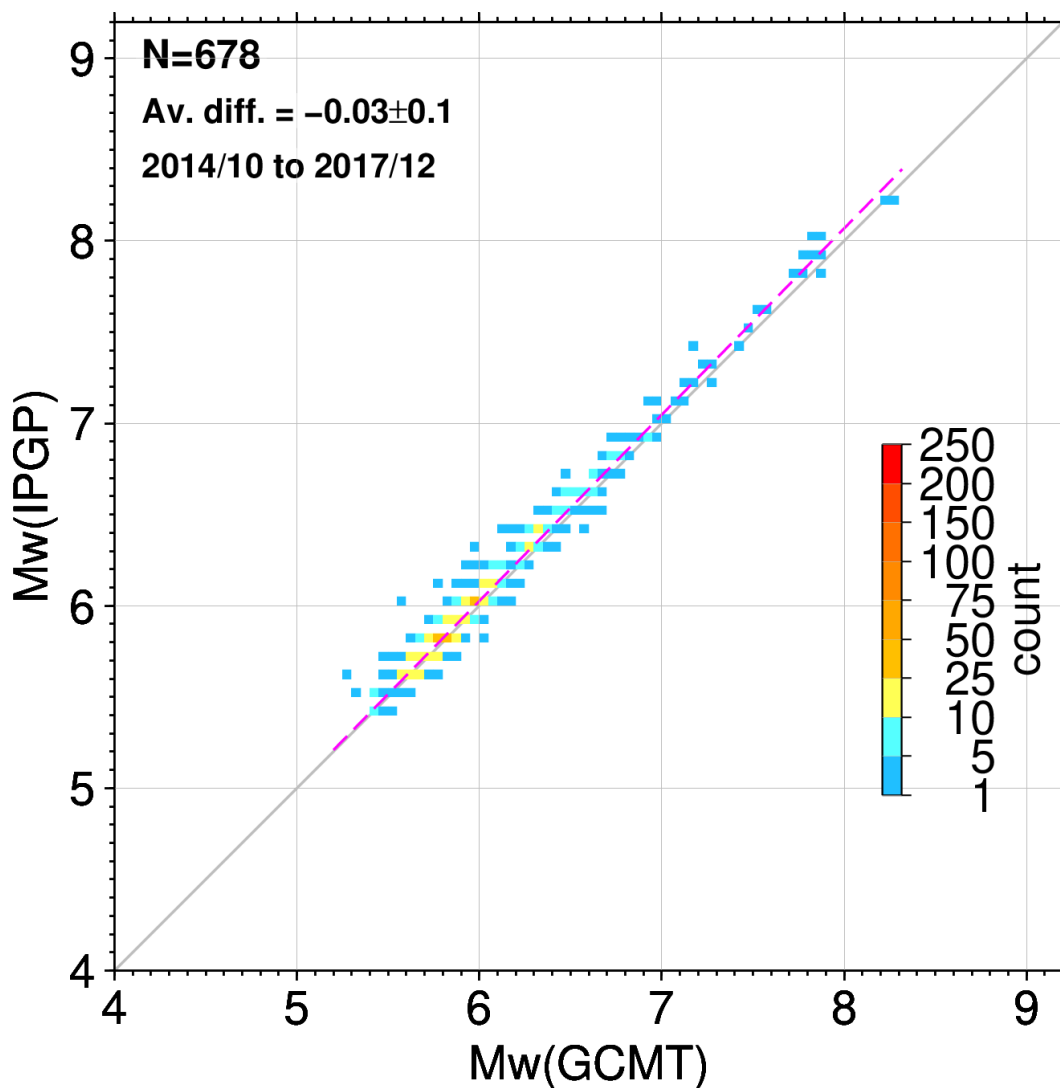
**Figure A17.** As for Fig. 8 but for GCMT and IPGP.
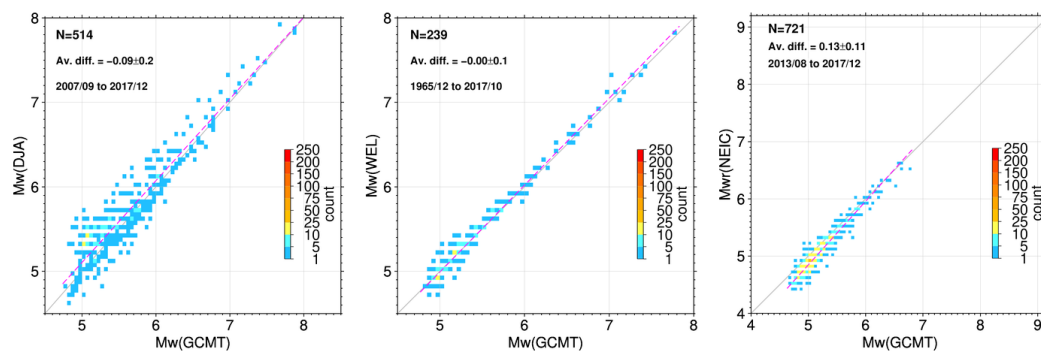
**Figure A18.** As for Fig. 8 but for GCMT and DJA (left), GCMT and WEL (middle), GCMT and *Mwr* NEIC (right).